Long-Range Forecasting and Climate Research

Simulation of the Madden and Julian Oscillation in GCM Experiments

by

R. Swinbank

LONDON, METEOROLOGICAL OFFICE.
Long-range Forecasting and Climate Research Memorandum
No. LRFC 14
Simulation of the Madden and Julian oscillation
in GCM experiments.

06200687 FH1B

LRFC 14

May 1987

LF/M013

LONG RANGE FORECASTING AND CLIMATE
RESEARCH MEMORANDUM NO. 14

Simulation of the Madden and Julian Oscillation in GCM Experiments

by

R SWINBANK

Met O 13 (Synoptic Climatology Branch)
Meteorological Office
London Road
Bracknell
Berkshire RG12 2SZ

May 1987

Simulation of the Madden and Julian Oscillation in GCM Experiments

by R Swinbank

1. Introduction

It is now well established that oscillations of a period between about 30 and 60 days occur in a variety of atmospheric variables, particularly in the tropics. The oscillation was first discovered by Madden and Julian (1971, 1972), who found variations in upper and lower troposphere wind, of opposite sense, on the 40 to 50 day time scale. (We refer to the phenomenon hereafter as the Madden and Julian, or MJ, oscillation). They interpreted these data in terms of an eastward propagating global scale convective cell in the equatorial plane. Other workers have found eastward propagating disturbances in outgoing longwave radiation data, which is an indicator of tropical convection (eg Lau and Chan, 1985). The clearest signal of the oscillation is found over the Indian and West Pacific Oceans; during the SW monsoon northward propagating areas of convection occur, which are related to the oscillation (Yasunari, 1980). There is also evidence that the MJ oscillation affects mid-latitudes. Weickmann (1983) and Weickmann et al (1985) have shown statistically significant relationships between the oscillation and mid-latitude atmospheric circulation.

In a recent paper Lorenc (1984) analysed velocity potential fields from the FGGE year using empirical orthogonal functions (EOFs). The main result was a description of an eastward propagating wave in the 200 mb divergent flow, with a zonal wavenumber 1 and period in the range 30-50 days. This was identified with the oscillations found by Madden and Julian. In the present paper, the same EOF technique has been applied to results from General Circulation Model (GCM) experiments. The first GCM experiment analysed is part of Met O 20 'third annual cycle' experiment, which is a long-running simulation with a standard version of the Met O 20 11-layer GCM (Slingo 1985) - see section 2. Hayashi and Sumi (1986) have found that the MJ oscillation can be simulated with an 'aqua-planet' model, in which all grid points in a GCM are treated as sea points, with sea surface temperatures independent of longitude. Lau and Peng (1986) have also simulated the MJ oscillation using a low resolution spectral GCM with a simple parametrization of convective heating. We have repeated Hayashi and Sumi's experiment, and extended their work to examine the dependence of the wave on latent heat release. These 'aqua-planet' experiments are described in section 3. The relationship between the model results and the observed MJ oscillations is discussed in section 4. Since other workers have reported that the MJ oscillations affect mid-latitudes, and periodicities on the same timescale as the MJ oscillation have been found in atmospheric angular momentum data, possible extra-tropical effects are investigated in section 5.

2. Results from an Annual Cycle GCM Experiment

In order to build up a model climatology, and to provide a control run for comparison with other experiments, Met O 20 have carried out a few multi-annual cycle GCM integrations. We have studied the simulation of the MJ oscillation in one of these integrations, the so-called 'third annual cycle' experiment. The physical parametrizations used in the experiment

have been described by Slingo (1985), and included the interactive radiation scheme (but with fixed cloud amounts). The experiment started from the Met Office level IIIa FGGE analysis for 25th July 1979. For this study, we have analysed the first four complete three month seasons (from September to August) for the MJ oscillations. The method used is similar to that used by Lorenc (1984) for analysing data for the FGGE year.

Daily velocity potential fields were calculated from the divergent wind at 200 mb

$$\chi(t) = \nabla^{-2}(\nabla.V(t))$$

The time-mean, annual and semi-annual cycles of the velocity potential were then calculated

$$\chi(t) = \chi + \chi_c \cos(wt) + \chi_s \sin(wt) + \chi_{c2} \cos(2wt) + \chi_{s2} \sin(2wt) + \chi_a(t)$$

where $w = 2\pi/\text{year}$ (for the model 1 year = 360 days). An EOF analysis was then carried out on the resulting time series, $\chi_a(t)$; no further time filtering was carried out. The EOFs were calculated as those functions χ_i which in turn minimized the global mean square variance of the residual $\chi_r(t)$, where

$$\chi_a(t) = \left(\sum_{i=1}^{N} C_i(t)\chi_i\right) + \chi_r(t)$$

For ease of computation all calculations were carried out using spectral representation triangularly truncated at T15.

Figure 1 summarizes the results of an EOF analysis of 250 mb velocity potential from the third annual cycle experiment (the 200 mb data were not available in this case). Figs. 1a and b shows the first two EOFs, which in each case are patterns of zonal wavenumber 1, of similar magnitude and are about 90° longitude different in phase. The time series of their coefficients (Fig. 1c) show periodicities of 20-40 days separated by about a quarter cycle in phase. This is clearest in the period November-April (approximately day numbers 100-280). Taken together these EOFs represent an eastward propagating planetary scale wave.

For comparison, an EOF analysis of analysed 200 mb velocity potential data has been carried out for data from the Met Office operational analyses for July 1984 to June 1985. The two leading EOFs and their coefficients are shown in Fig. 2. Once again they describe an eastward propagating wavenumber 1 feature. However the period of the wave is 30 to 50 days. These results are similar to those found by Lorenc (1984) for the FGGE year (December 1978 to November 1979). R Bromley (private communication) has pointed out variations in atmospheric angular momentum data which are similar to the variations in the EOF coefficients in Fig. 2. This indicates a link between the tropical MJ oscillations and variations in angular momentum on the same time scale; this notion is explored further in section 5.

These results show that a general circulation model is capable of simulating the MJ oscillations found in the atmosphere, though the GCM simulation has produced a reduction in the period of the wave, indicating some shortcomings in the model simulation.

3. Aqua Planet Simulations

Hayashi and Sumi (1986) reasoned, from observational evidence, that the MJ oscillation is a result of an interaction between the large scale flow and tropical convection over the ocean with a region of high SSTs (such as the western Pacific). Further, they argued that an idealised form of the MJ oscillation would be realised if the whole globe were covered with a zonally uniform ocean. In such a system, convection would occur on the super-cluster scale (of about 3000 km) and move eastward coherently. Accordingly, they carried out GCM experiments using a model in which the whole surface is covered with an ocean (which they dubbed an 'aqua planet'). As they had speculated, they found that the model generated an eastward propagating wave 1 structure, which was linked with variations in the convection. The wave propagated eastwards with a phase speed of 15 m/s (corresponding to a period of 30 days).

We have repeated Hayashi and Sumi's experiment with an 'aqua-planet' version of the Met O 20 11-layer model. The initial data was derived from the Met Office operational analysis for 00Z 26/3/85. The surface pressure was adjusted to sea level, then all the model fields were zonally meaned and also meaned between the hemispheres, so that the southern hemisphere circulation was as for the northern hemisphere, reflected in the equatorial plane. The sea surface temperature was calculated in a similar manner, but omitting surface temperatures from points that were originally land points. All sea ice points (and points under Antartica) were treated as sea points with a temperature of 272K. The resulting SSTs are shown in Fig. 3 (also shown are the SSTs for another experiment described later in this section). The radiation scheme used in the experiments was the climatological scheme with parameters fixed for 21st March - the spring equinox. (The radiative forcing was not quite hemispherically symmetric because of different assumed zonally symmetric cloud distributions in the two hemispheres). Thus the only forcing that can disturb zonal symmetry is provided by the diurnal cycle in radiative heating. The experiment has been run for a period of 90 days from the initial data.

Before showing diagnostics of the MJ oscillation, we shall briefly describe some unusual aspects of the time-mean fields from this experiment. Fig. 4 shows the distribution of zonal-mean rainfall and 850 mb wind for days 61 to 90. There are two principal rainfall bands, one in each hemisphere at about 15° from the equator, with a relative minimum at the equator. Approximately coincident with the rainfall bands there are easterly low level winds, with very weak zonal mean flow at the equator. In the extratropics, there are westerly maxima at about 45°N and S. These features reflect the absence of topographic and thermal forcing by land-sea contrasts. In the tropics, the zonal mean meridional circulation shows a pair of Hadley cells with ascending branches coinciding with the rain bands. Between the rain bands the meridional circulation is very weak, with a hint of descent over the equator. The reason for this circulation pattern appears to be related to differences between eddy momentum fluxes simulated by the aqua planet model and those observed in the atmsophere.

The poleward shift of the Hadley cells is associated with a poleward shift of the momentum flux divergence; this in turn is a result of the almost complete absence of stationary wave fluxes in the aqua planet (for further details see Swinbank et al, 1987).

In Figs. 5 and 6 the results of an EOF analysis of the 200 mb velocity potential are presented. Since this experiment was at a fixed time of year, no annual or semi-annual cycle was subtracted. (In these and subsequent 'aqua-planet' maps the coastlines have no significance, other than an indicator of scale and orientation). As found in the 'annual cycle' experiment (section 2), the two leading EOFs (Fig. 5) describe an eastward propagating wave 1 disturbance. Because of the greater simplicity of the model, the results are much clearer than for the previous experiments. EOFs 3 and 4 are shown in Fig. 6, together with their coefficient time series. This shows that a further component of the MJ oscillation is described by a wave 2 disturbance travelling eastward with approximately the same phase speed as the wave 1 feature. Thus the eastward propagating disturbance is not a simple wave 1 feature but incorporates at least wave 2 scale as well; the wave 1 nature of the phenomenon shown by EOFs 1 and 2 is largely an artifact of the EOF analysis. The period of the oscillation in this experiment has been reduced to about 20 days.

Figure 7 shows Hovmoller diagrams of the 200 mb velocity potential and convective rainfall. It can be clearly seen that at about day 30 an eastward propagating disturbance appears in the velocity potential that persists to the end of the integration, as one would infer from the EOF analysis. A spectral analysis confirms that the wavenumber one component of the disturbance has a period of 20 days, corresponding to a phase speed of about 23 ms^{-1}. The Hovmoller diagram for convective rain (Fig. 7b) shows, naturally, smaller scale features. Around day 10 convective rain breaks out about every 45 degrees of longitude. Each outbreak propagates eastward at a rate of about 4° per day. It is possible that these rain areas are responsible for forcing the large scale disturbance in velocity potential which starts to appear about day 20. In turn, the large scale divergence pattern has a modulating influence on the rainfall in later stages of the integrations. As well as this eastward moving modulation, there are westward propagating features in the rainfall. These westward propagating features are not so apparent in the velocity potential data. We note in passing that, during the period 1985/6, a strong 25-35 day eastward propagating disturbance in velocity potential was observed. A Hovmoller diagram of outgoing longwave radiation, however, showed some westward propagating features in addition to the eastward moving features (see WCP, 1986).

Returning to the velocity potential diagram (Fig. 7a), the zero contour (corresponding to 200 mb westerlies, ie. the upper edge of the shaded regions in the diagram) progresses very smoothly in the latter part of the integration. The longitude of this contour has been used to define the phase of the wave for any particular day. Composites of various model fields for days 61 to 90 have been calculated relative to the wave (ie. the fields were shifted in longitude so that the apparent phase of the wave is zero). Figure 8 shows composites of the 200 mb and 850 mb wind fields (with zonal means subtracted for clarity). The vertical structure is shown in Fig. 9, which is a cross-section in the equatorial plane of the composite wind fields. This indicates that the maximum westerly anomaly is

between 150 mb and 200 mb, with an associated easterly anomaly at 850 mb. On the western side of the wave there is a region of quite strong ascent at the equator, which is linked with enhanced convective rain; conversely on the eastern side descent is associated with reduced rainfall. Maps of the convective rain and vertical velocity composites are given in Fig. 10. It is also apparent that there is a significant enhancement of the twin rainfall bands, again associated with increased ascent (cf Fig. 4).

The structure is consistent with an atmospheric Kelvin mode, however the phase speed is much less than one would expect for a wave with this structure (eg. Gill 1982, Chapter 11). Experiments with a simple moist model of the tropical atmosphere (Davey and Gill, 1986; Swinbank et al 1987) demonstrate that the phase speed of a Kelvin wave can be reduced by moisture effects. Latent heat release from areas of active precipitation associated with the wave reduces the static stability and so also reduces the phase speed. It is interesting to note that Madden and Julian (1971) considered the possibility that the phenomenon was basically an atmospheric Kelvin wave; however they dismissed the possibility when they were unable to reconcile the characteristics of the wave with theory. Chang (1977) proposed an explanation of the MJ oscillation as a Kelvin wave, with the period of the wave modified by a large dissipation term. Lau and Peng (1986) have recently suggested that the oscillation is a Kelvin wave modified by a wave CISK mechanism.

We have tested the notion that the wave speed is sensitive to latent heat release with two further GCM experiments. In the first of these experiments the latent heat release was increased by increasing the tropical sea surface temperature, so increasing the amount of convective rain. An increment of 1 K was added to the SST for the eight model rows between 10°N and 10°S; this increment was decreased by 0.25 K for each subsequent row until it reached zero. The original and modified SSTs are shown in Fig. 3. In the other experiment the latent heat release is increased by simply doubling the value of the latent heat of evaporation used by the model; this does not double the latent heat release, since there is also some reduction in the rainfall amounts.

Graphs of zonal mean rainfall and 850 mb wind for the second and third experiments are given in Figs. 11 and 12 respectively. Compared to the first experiment (Fig. 4), the increased tropical SSTs in the second experiment have markedly increased the intensity of the rainfall bands at 15°N and 15°S, and shifted their position towards the equator; between 15°N and 15°S the total rainfall has been increased by about 40%. There is also an increase in the strength of the 850 mb easterlies associated with the rain bands. In the third experiment there is a general decrease in the rainfall, with the magnitude reduced by about 30% within 15° of the equator; since the latent heat constant has been doubled this represents a 40% increase in the latent heat release. Interestingly (and contrary to our prior expectations) this has not resulted in an intensification of the equatorial meridional circulation, but rather a weakening of the circulation in the third experiment as compared to the first. The enhanced latent heating has warmed the upper tropical troposphere, by about 25K at 200 mb; it appears that increased radiative cooling as a result of this warming has compensated, in the thermodynamic equation, for the latent heat

release, with no increase in cooling by adiabatic ascent. As a result of this warming, the tropopause level has been raised, together with the sub-tropical jets and upper branches of the Hadley circulation.

Hovmoller diagrams of the 150 mb velocity potential for the three experiments are shown in Fig. 13. The results for the first experiment at 150 mb are very similar to the 200 mb data (Fig. 7a). In the second experiment a disturbance, similar to that found in the first experiment, appears about day 30 and, apart from some disruption about day 45, it continues to the end of the integration. A spectral analysis shows that the wavenumber one component of this disturbance has a period of 25 days. In the third experiment a somewhat weaker and less coherent eastward propagating disturbance can be seen in the Hovmoller diagram (Fig. 13c). Visual inspection suggests that the period of the disturbance has increased to 30 days. (For example, the unshaded region near the Greenwich meridian on day 25 appears to be coherent for one complete period, returning to the Greenwich meridian about day 55). Spectral analysis shows a weak wavenumber 1 peak at 30 days.

From composites of all three experiments we have calculated equivalent potential temperature, θ_e, values for a region within 15° latitude of the equator and $22^1/_2$° longitude of the upper level westerly wind maximum. Profiles of θ_e as a function of pressure are shown in Fig. 14. Comparison of the θ_e values with θ_e^* (equivalent potential temperature of a saturated atmosphere with the same temperature structure) show that all three profiles exhibit conditional instability, confirming that convection can readily occur in each case. We have taken the difference between the equivalent potential temperature at low levels and the mid-troposphere as an indication of effective static stability; comparison of Fig. 14 with the wave periods mentioned above indicates that the more unstable the atmosphere, the slower the speed of the MJ oscillation. The relationship between the intrinsic wave speed, allowing for changes in the basic state flow, and static stability is shown in more detail in Table 1. In this table the wave speed (adjusted using the 700 mb westerly flow) is shown to be approximately inversely proportional to an effective Brunt-Vaisala frequency, as estimated from the difference in θ_e between 1000 mb and 700 mb.

4. Discussion

Perhaps the most obvious difference between the observed MJ oscillations and the oscilltions simulated with the 11-layer GCM is that the simulated wave period is too short. It has been shown that the wave speed is sensitive to the effect of latent heat release, so a likely explanation is that this is insufficiently well represented in the model. M Blackburn (private communication) has found that the wave speed of a tropical Kelvin wave disturbance is sensitive to the model convection scheme. It is probable that changing the convection scheme used in the 11 layer model would change the effective static stability and may produce better simulations of the period of the MJ oscillation. Lau and Peng (1986) have also simulated the MJ oscillation in a numerical model, and found that the model disturbance propagates about twice as fast as observed. Their analysis suggests that the propagation speed is related to that of the dominant model normal mode, as modified to take into account the effect of latent heat release. Thus the wave speed depends on the

equivalent depth of the appropriate model vertical mode, which may not correspond to the effective equivalent depth of the observed MJ oscillation.

In addition, the zonal symmetry of the 'aqua planet' experiments affects the wave period; a period of about 30 days was found in the 'third annual cycle' experiment (section 2), while for the basic aqua planet experiment the period was about 20 days (section 3). One would expect that the period of a Kelvin wave would be reduced when travelling through regions of enhanced convective activity. The MJ oscillation has been studied by various workers (eg Lau and Chan 1985, Weickmann et al 1985), using outgoing long-wave radiation data from satellites. The signal of the wave in the OLR data is clearest over the Indian and West Pacific Oceans, where the SSTs are relatively warm and convective activity is relatively strong. Weickmann et al found a reasonably uniform progression of large scale OLR anomalies from 60°E to 160°E, but a less uniform (but faster) progression at other longitudes. (Knutson and Weickmann (1986) show that, although the OLR anomalies are mainly confined to the Indian Ocean/W Pacific sector, the corresponding circulation anomalies progress more smoothly around the whole tropics). It is not immediately clear exactly how the wave period depends on the zonal asymmetry, but these considerations indicate that one would not necessarily expect the 'aqua-planet' experiments to simulate waves of the period actually observed.

The speed of the wave will also be affected by the speed of the basic flow through which the wave is travelling. Some possible observational evidence which confirms this is provided by an extended EOF analysis of OLR data by Lau and Chan (1985). They found an eastward progression of waves between the Indian and West Pacific Oceans, which tend to become virtually stationary over the W Pacific. This may correspond to an eastward propagating disturbance whose speed is reduced when it encounters the generally westerly low level flow in the W Pacific.

The disturbances found in the first two aqua-planet experiments are relatively small in longitudinal extent and progress quite steadily. However, in the atmosphere the MJ oscillations are much less regular. This can be partly attributed to variations in the factors mentioned above (eg sea surface temperature and tropical wind fields), but the third aqua-planet experiment shows that, even with zonally symmetric forcing, the wave can be disrupted quite easily. It has also been found that the regularity of the wave is spoiled by using the interactive radiation scheme instead of the climatological scheme.

5. Extra-tropical connections

An important aspect of the MJ oscillation is its effects on the extra-tropics. As already mentioned, Weickmann (1983) and Weickmann et al (1985), among others, have shown a connection between the tropical oscillation and mid-latitude atmospheric circulation. Langley et al (1981) have found variations in atmospheric angular momentum (and corresponding slight changes to the length of day) on the 40-50 day timescale. The latitude-height structure of these angular momentum fluctuations has been studied by Anderson and Rosen (1983), who concluded that these fluctuations were related to the MJ oscillation.

The Kelvin mode, which we have taken as a model for the MJ oscillation, is restricted to an equatorial waveguide, of width scale the operational Rossby radius (about 700 km). One would expect that the wave would affect mid-latitudes largely through interaction with zonal asymmetries, such as land-sea contrast, orography and SST variations, by Rossby wave-trains propagating into mid-latitudes. In order to study the effects of one such zonal asymmetry, we have run an experiment which reintroduces land-sea contrast into the 'aqua planet' model; we denote this the 'flat land' model. Instead of all grid points being sea points, the normal land-sea distribution is used, but with no orography (strictly, all land points have an elevation of 1 m). The initial land surface temperature is as for the sea surface and the initial soil moisture content is 5 cm of water. All other parameters are as for the standard aqua planet experiment.

A Hovmoller diagram of the tropical velocity potential at 200 mb is shown in Fig. 15; in this case the time-mean has been subtracted. The 'flat land' experiment clearly exhibits the MJ oscillation. Its period has been increased slightly to about 22 days, consistent with the discussion in section 4. The disturbance itself is spread out along a greater longitude range than in the aqua planet experiments (compare Fig. 7 with Fig. 15); in this respect it is more similar to the observed MJ oscillation.

As demonstrated by Fig. 16a, the extra-tropical eddy kinetic energy (KE) exhibits variations on the same time-scales as the MJ oscillation. To a small degree, the variations in eddy KE are compensated by opposite variations in the zonal KE. (This data is calculated just from model fields at 200 mb, but should be representative of the upper troposphere/lower stratosphere of the model, where the wind is generally of largest magnitude). Fig. 16b shows variations of the relative angular momentum (actually the zonal wind multiplied by the cosine of the latitude). Variations in the angular momentum (AM) are well correlated with the fluctuations in eddy and zonal kinetic energy. For comparison, the variations of the MJ oscillation are also indicated, in terms of when the maxima and minima of tropical velocity potential occur at the Greenwich meridian. This shows that there is a reasonable correlation between the MJ oscillation and mid-latitude variations of AM and KE. Figure 16 shows data just from the northern hemisphere; equivalent southern hemisphere data is in Fig. 17. This shows that similar variations occur in the southern hemisphere, but note that the oscillations in each hemisphere are of opposite phase.

The same quantities are plotted for the basic aqua-planet experiment in Fig. 18. After an initial settling down period, the aqua planet run exhibits a similar kinetic energy 'index cycle' to that of the flat land model, but with a small amplitude and more variability at shorter periods. The angular momentum does not show very clear fluctuations; after the initial 20 days the main trend is a gradual increase, though there are some slight oscillations that may be linked to those in the KE data. In this case there again appears to be a correlation between the kinetic energy and the MJ oscillation phase. This is unexpected since the aqua planet model is zonally symmetric, so there should be no coupling between the simulated

MJ oscillation and a zonally meaned quantity such as the eddy kinetic energy. Thus the two sets of mid-latitude and tropical variations must be independent in this model, although of similar period.

Figure 19 shows the kinetic energy and angular momentum data from the 'third annual cycle' experiment, for the period when the MJ oscillation was strongest (see Fig. 1c). Again the phase of the oscillation is indicated (this time using the EOF1 coefficient); there is no clear correlation with the fluctuations in KE and AM. All these results show that the GCM integrations exhibit mid-latitude variability on the same time scale as the tropical MJ oscillation, but do not show that the two sets of variations are connected. While the variations are apparently independent in the 'aqua planet' model and in the 'third annual cycle' experiment, it does not necessarily follow that the two do not interact in the real atmosphere.

This study does not extend to an invetigation of the mechanisms of these mid-latitude oscillations. James and Gray (1986) report fluctuations in the eddy kinetic energy, which are similar to those found in the present study, in hemispheric spectral model experiments. They attributed the variations to a 'barotropic governor' mechanism. In this scenario an initial rapid conversion from zonal available potential energy to eddy KE results in an outburst of eddy activity. Large conversions to zonal KE follow and an appreciable barotropic component is added to the mean zonal flow, which then becomes more stable to baroclinic conversions. As a result the level of eddy activity declines and the available potential energy is allowed to build up again. In certain cases this can lead to the type of vacillatory or 'index cycle' behaviour seen in the present experiments. The period of the oscillations in their experiments tended to decrease as the surface drag was reduced; this is consistent with the shorter period fluctuations of KE found in the aqua planet experiment (interestingly, they also found that in the low drag experiments the Hadley cell became a weak indirect circulation). James and Gray did not report any variations in the simulated angular momentum. At present there does not appear to be an accepted theory to account for the intra-seasonal oscillations of AM. Swinbank (1985) showed that, in the atmosphere and in realistic general circulation models, the AM fluctuations are mainly associated with changes in the mountain torque, while the torque resulting from boundary layer stress varies insufficiently on a large scale. However, in the current experiments there is no mountain torque possible; instead it appears that angular momentum is exchanged between the hemispheres.

6. Conclusions

The general circulation model experiments described in this paper exhibit oscillations that are similar in nature to the eastward propagating MJ waves that are found in the atmosphere. The fact that these disturbances are found in 'aqua planet' integrations demonstrates that neither topographic nor land-sea contrasts are crucial to the basic mechanism of the phenomenon. The structure of the disturbance in the GCM resembles a Kelvin waves, but its speed of propagation is less than one would expect from simple theory. However it has been demonstrated that the wave speed is sensitive to moisture effects. This was shown by a pair of GCM simulations in which the latent heat release was increased, firstly by increasing the sea surface temperature and secondly increasing the latent

heat constant. Although neither the aqua planet experiments nor a more realistic experiment simulate a long enough wave period, this is likely to be because of shortcomings in the parametrization of convection.

It has also been demonstrated that the GCM exhibits mid-latitude variability on the same timescale as the MJ oscillation. However this study does not include an investigation of the mechanisms of the scope of this extra-tropical variability and how it may be linked to the MJ oscillation. This topic should be a fruitful area for future study.

References

Anderson, J.R. and Rosen, R.D. 1983 The latitude height structure of 40-50 day variations in atmospheric angular momentum. J. Atmos. Sci., 40, 1584-1591.

Chang, C-P 1977 Viscous internal gravity waves and low frequency oscillations in the tropics. J. Atmos. Sci., 34, 901-910.

Chiba, M. 1986 Long term fluctuation of the tropical atmsophere simulated by the low resolution spectral GCM. Workshop on 40 day mode and ENSO. Meteorological Research Report 86-1 Division of Meteorology, Geophysical Institute, University of Tokyo.

Davey, M.K. and Gill, A.E. 1986 Experiments on tropical circulation with a simple moist model. Dynamical Climatology Technical Note No. 41, Meteorological Office, Bracknell.

Gill, A.E. 1982 Atmosphere-Ocean Dynamics. International Geophysics Series, Vol 30, Academic Press, 662 pp.

Hayashi, Y.-Y., and Sumi, A. 1986 The 30-40 day oscillations in an 'aqua-planet' model. J. Met. Soc. Japan. II, 64, 451-467.

James, I.N. and Gray, L.J. 1986 Concerning the effect of surface drag on circulation of a baroclinic planetary atmosphere. Quart. J. R. Met. Soc., 112, 1231-1250.

Knutson, T.R., and Weickmann, K.M. 1986 30-60 day atmospheric oscillations: composite life cycles of convection and circulation anomalies. Mon. Wea. Rev. (submitted).

Langley, R.B., King, R.W., Shapiro, I.I. and Rosen, R.D. 1981 Atmospheric angular momentum and the length of day: a common fluctuation with a period near 50 days. Nature, 294, 730-732.

Lau, K.M. and Chan, P.H. 1985 Aspects of the 40-50 day oscillation during the northern winter as inferred from outgoing longwave radiation. Mon. Wea. Rev., 113, 1889-1909.

Lau, N-C., and Lau, K-M. 1986 The structure and propagation of intraseasonal oscillations appearing in a GFDL GCM. J. Atmos. Sci., 43, 2023-2047.

Lau, K.M. and Peng, L.	1986	Origin of low frequency (intraseasonal) oscillations in the tropical atmosphere. Part I: the basic theory. J. Atmos. Sci. (submitted).
Lorenc, A.C.	1984	The evolution of planetary-scale 200 mb divergent flow during the FGGE year. Quart. J. R. Met. Soc., 110, 427-441.
Madden, R.A. and Julian, P.R.	1971	Detection of a 40-50 day oscillation in the zonal wind in the tropical Pacific. J. Atmos. Sci., 28, 707-708.
Madden, R.A. and Julian, P.R.	1972	Description of global scale circulation cells in tropics with a 40-50 day period. J. Atmos. Sci., 29, 1109-1123.
Slingo, A. (Ed.)	1985	Handbook of the Meteorological Office 11-layer atmospheric model, Vol 1: Model Description. Dynamical Climatology Technical Note No. 29, Meteorological Office, Bracknell.
Swinbank, R., Palmer, T.N. and Davey, M.K.	1987	Numerical simulations of the Madden and Julian oscillation. J. Atmos. Sci. (submitted).
WCP	1986	Climate System Monitoring Monthly Bulletin, Issue No. 1986-3, March. World Climate Data Programme, WMO, Geneva.
Weickmann, K.M.	1983	Intraseasonal circulation and outgoing longwave radiation modes during Northern Hemisphere winter. Mon. Wea. Rev., 1838-1858.
Weickmann, K.M Lussky, G.R. and Kutzbach, J.E.	1985	Intraseasonal (30-60 day) fluctutions of outgoing longwave radiation and 250 mb streamfunction during northern winter. Mon. Wea. Rev., 113, 941-961.
Yasunari, T.	1980	A quasi-stationary appearance of the 30-50 day oscillation in the tropics. J. Met. Soc. Japan, 62, 709-717.

TABLE 1

Wave speeds for aqua-planet experiments.

	Standard Experiment	Increased SST	Doubled latent heat constant
Wave speed (ms^{-1})	22.0	17.8	15.4
U_{700}-averaged from 10°N to 10°N	-0.9	-3.0	-1.3
'Doppler shifted' wave speed	22.9	20.8	16.7
Ratio of wave speeds	1	1.10	1.37
$\theta_{e1000}-\theta_{e700}$	11.1	12.5	19.8
$\sqrt{(\Delta\theta_e)}$	3.34	3.54	4.45
Ratio of $\sqrt{(\Delta\theta_e)}$	1	1.06	1.33

Figure 1

a. THIRD ANNUAL CYCLE EXPERIMENT
250 MB VELOCITY POTENTIAL EOF 1 = SQRT(E-VALUE)

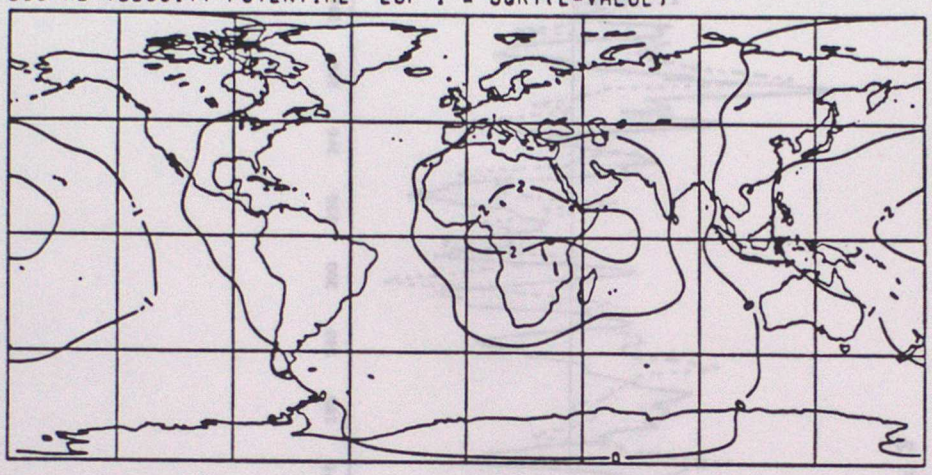

b. THIRD ANNUAL CYCLE EXPERIMENT
250 MB VELOCITY POTENTIAL EOF 2 = SQRT(E-VALUE)

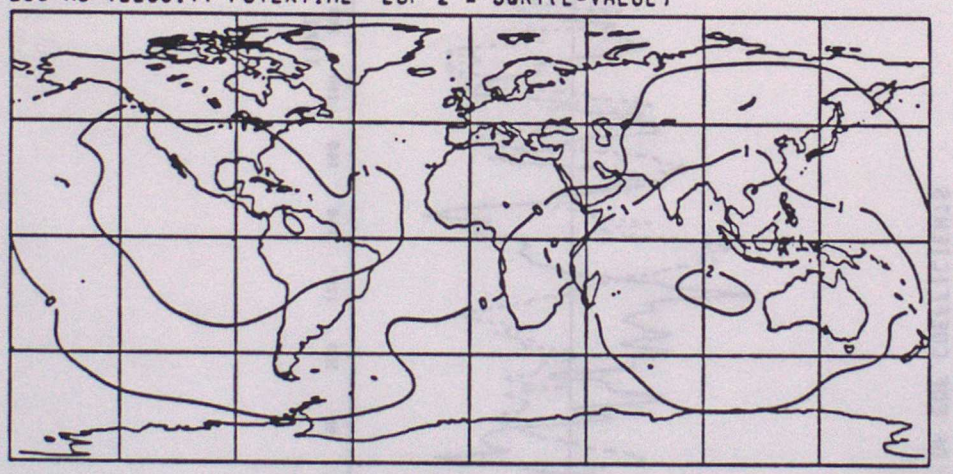

Figure 1c

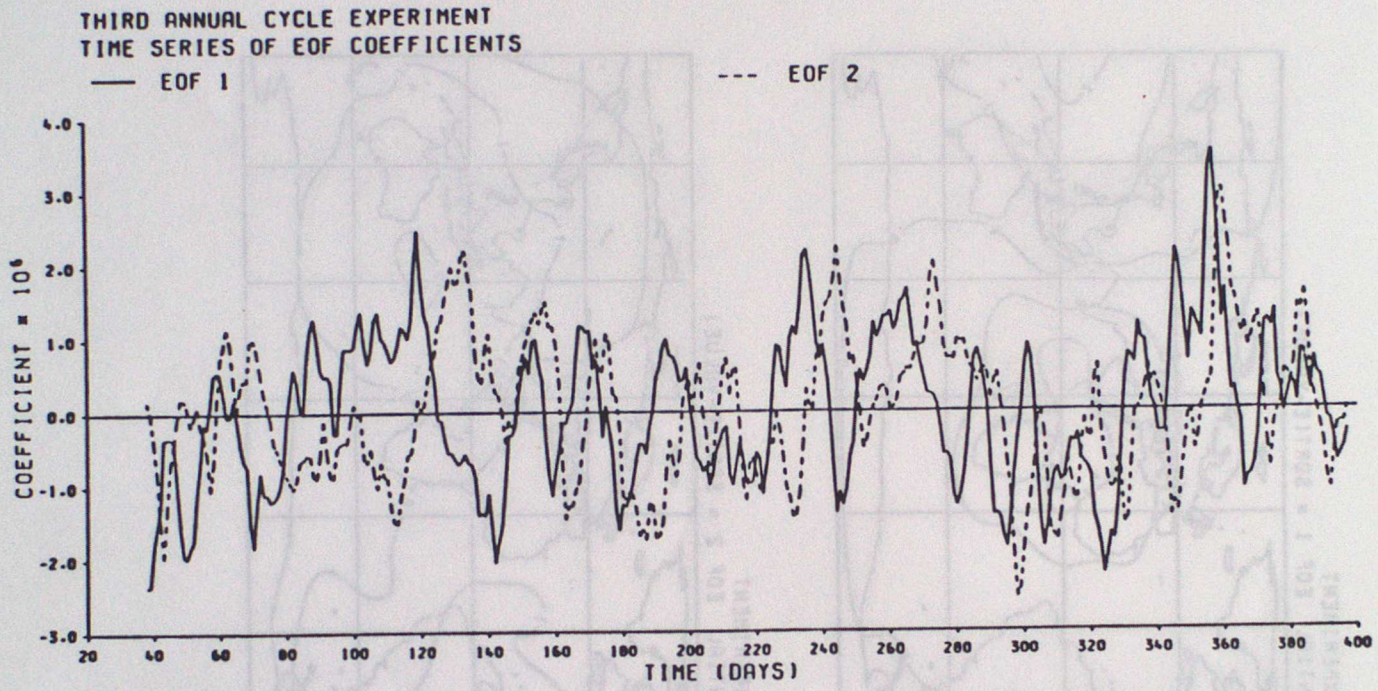
THIRD ANNUAL CYCLE EXPERIMENT
TIME SERIES OF EOF COEFFICIENTS
EOF 1
EOF 2
COEFFICIENT * 10⁶
4.0
3.0
2.0
1.0
0.0
-1.0
-2.0
-3.0
20
40
60
80
100
120
140
160
180
200
220
240
260
280
300
320
340
360
380
400
TIME (DAYS)

Figure 2

a. JULY 1984 - JUNE 1985
200 MB VELOCITY POTENTIAL EOF 1 = SQRT(E-VALUE)

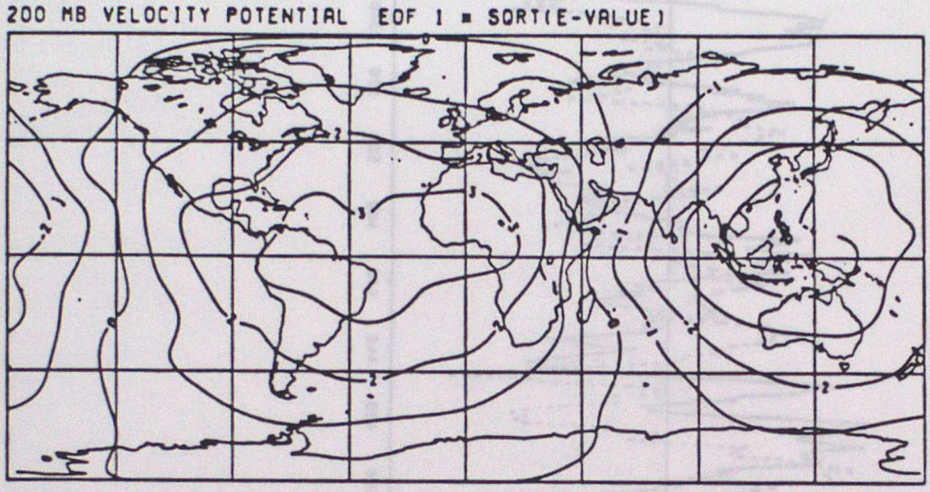

b. JULY 1984 - JUNE 1985
200 MB VELOCITY POTENTIAL EOF 2 = SQRT(E-VALUE)

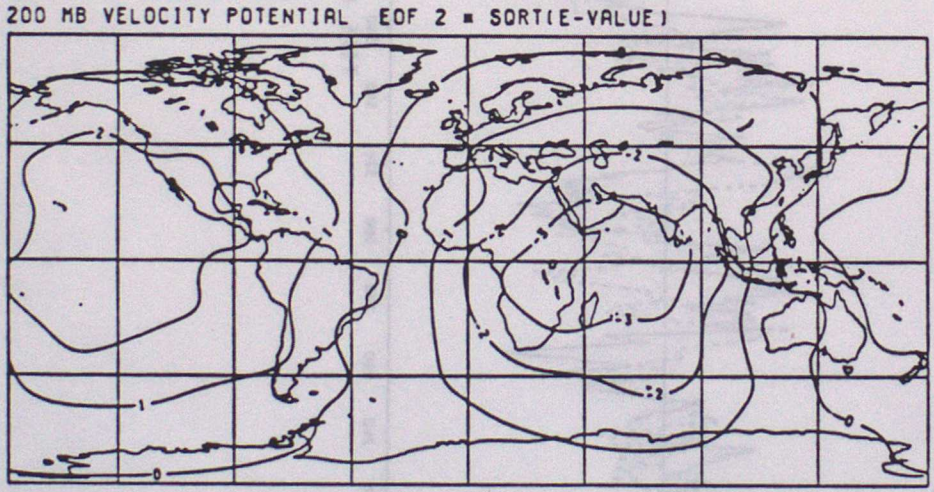

Figure 2c

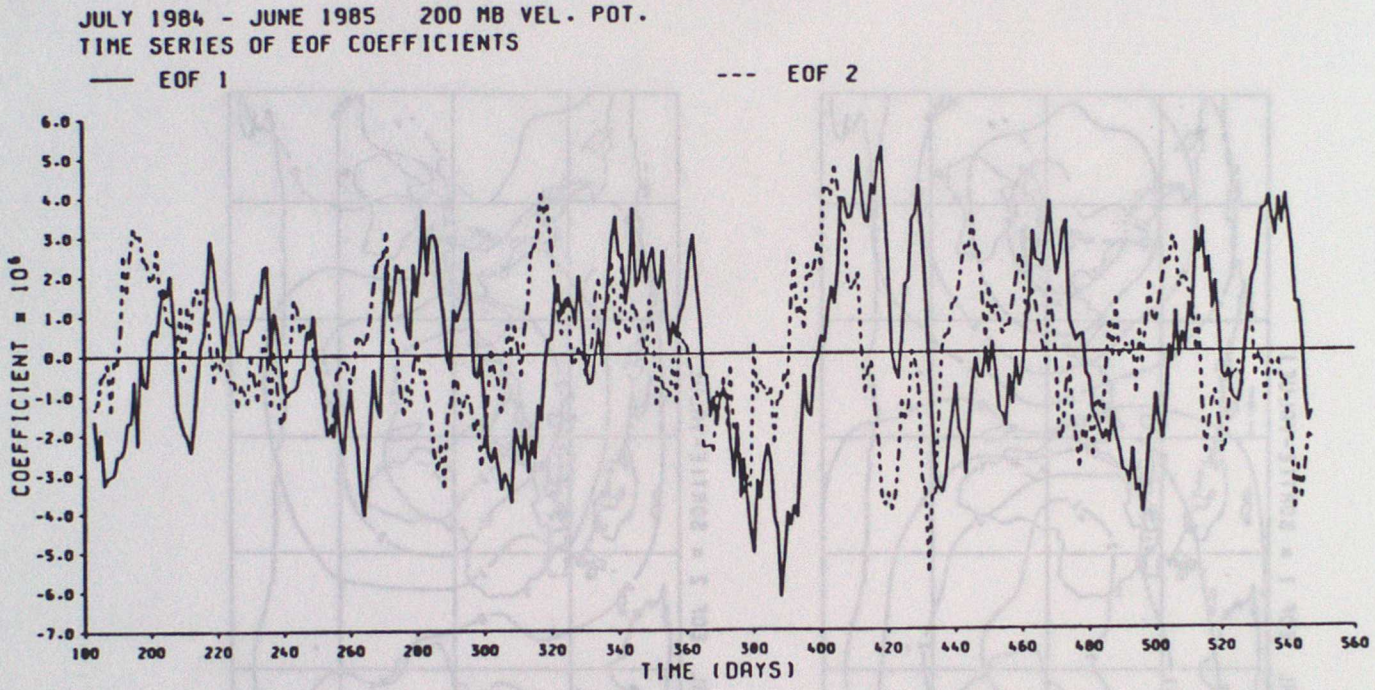
JULY 1984 - JUNE 1985 200 MB VEL. POT.
TIME SERIES OF EOF COEFFICIENTS
EOF 1
EOF 2
COEFFICIENT = 10⁶
6.0
5.0
4.0
3.0
2.0
1.0
0.0
-1.0
-2.0
-3.0
-4.0
-5.0
-6.0
-7.0
180
200
220
240
260
280
300
320
340
360
380
400
420
440
460
480
500
520
540
560
TIME (DAYS)

Figure 3

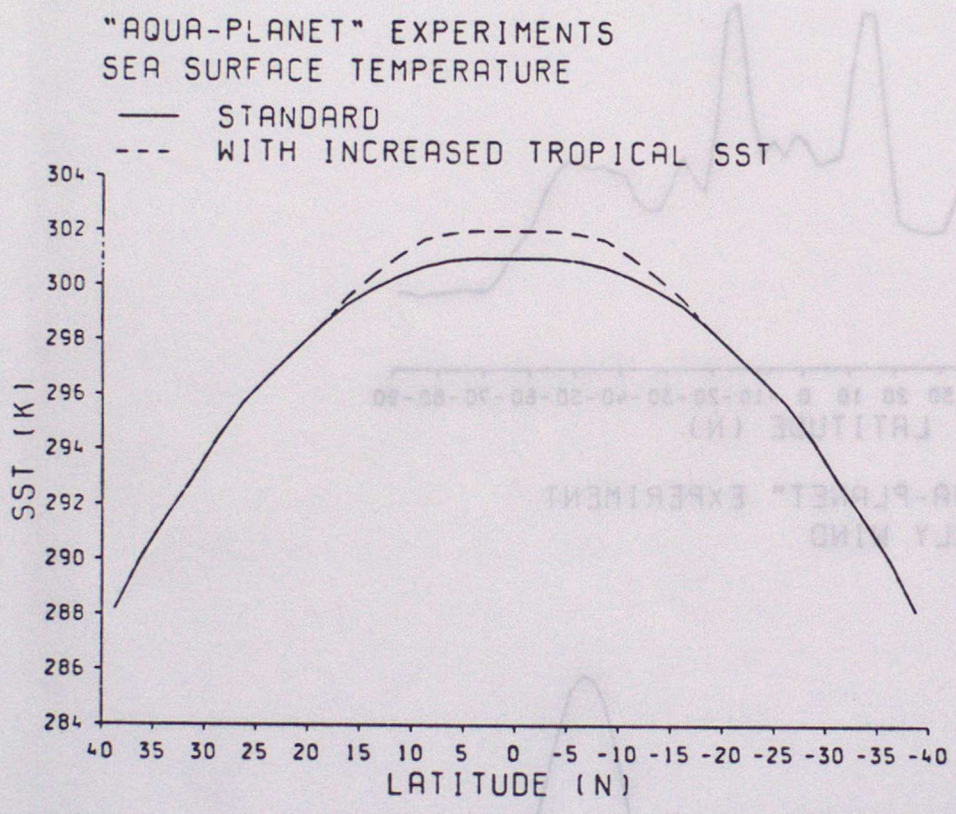
"AQUA-PLANET" EXPERIMENTS
SEA SURFACE TEMPERATURE
STANDARD
WITH INCREASED TROPICAL SST
SST (K)
304
302
300
298
296
294
292
290
288
286
284
40 35 30 25 20 15 10 5 0 -5 -10 -15 -20 -25 -30 -35 -40
LATITUDE (N)

Figure 4

STANDARD "AQUA-PLANET" EXPERIMENT
PRECIPITATION

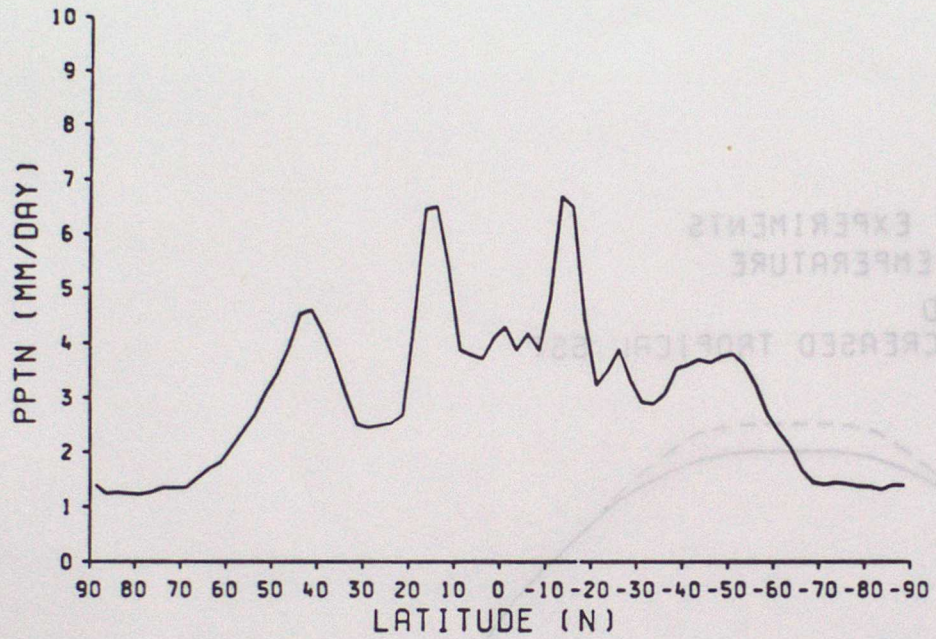

STANDARD "AQUA-PLANET" EXPERIMENT
850 MB WESTERLY WIND

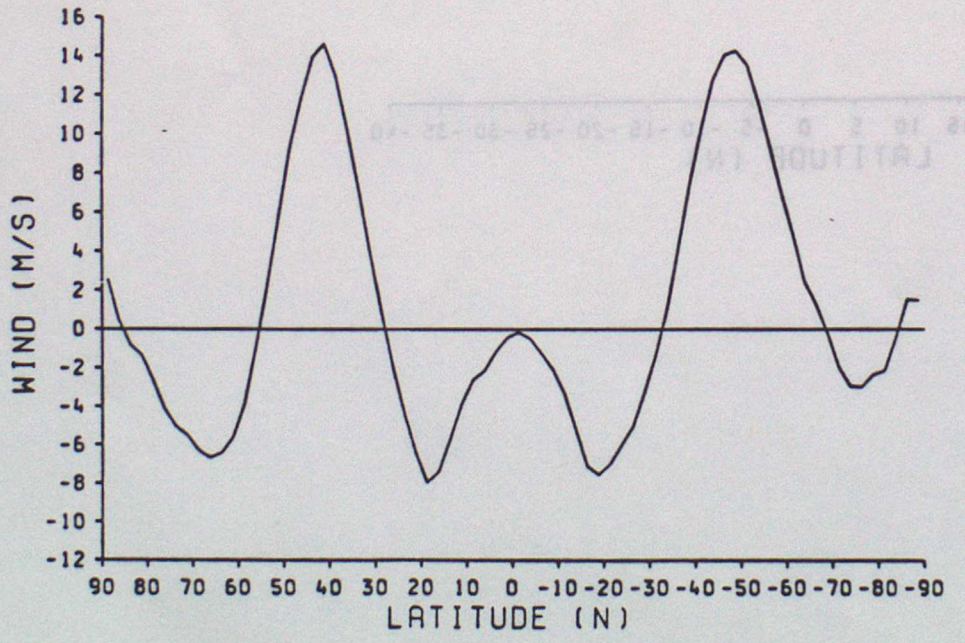

Figure 5

a. "AQUA-PLANET" EXPERIMENT
200 MB VELOCITY POTENTIAL EOF 1 = SQRT(E-VALUE)

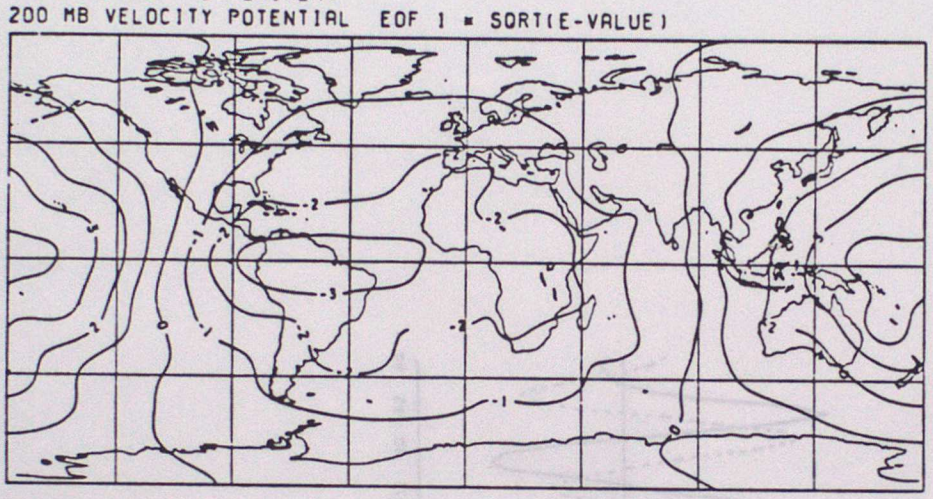

b. "AQUA-PLANET" EXPERIMENT
200 MB VELOCITY POTENTIAL EOF 2 = SQRT(E-VALUE)

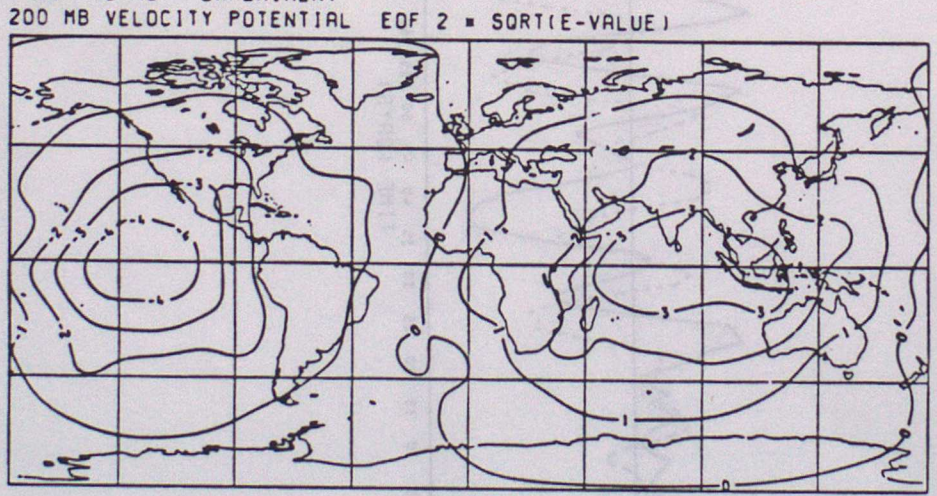

Figure 5c

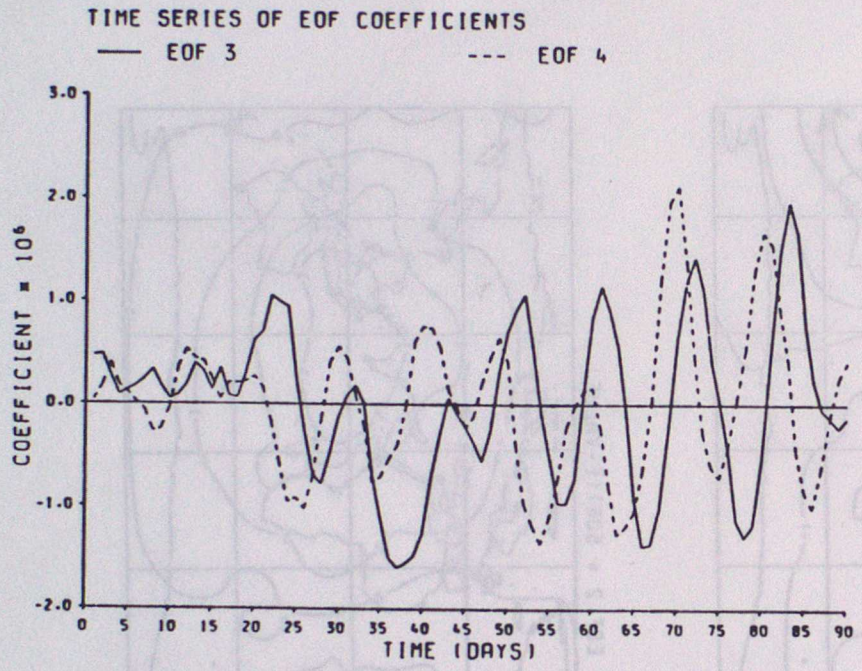
TIME SERIES OF EOF COEFFICIENTS
EOF 3
EOF 4
COEFFICIENT x 10⁶
3.0
2.0
1.0
0.0
-1.0
-2.0
0 5 10 15 20 25 30 35 40 45 50 55 60 65 70 75 80 85 90
TIME (DAYS)

Figure 6

a. "AQUA-PLANET" EXPERIMENT
200 MB VELOCITY POTENTIAL EOF 3 * SQRT(E-VALUE)

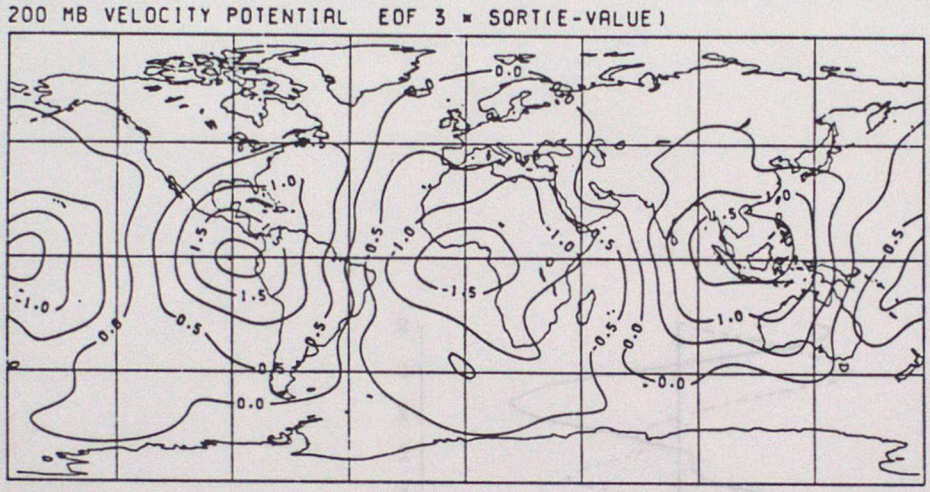

b. "AQUA-PLANET" EXPERIMENT
200 MB VELOCITY POTENTIAL EOF 4 * SQRT(E-VALUE)

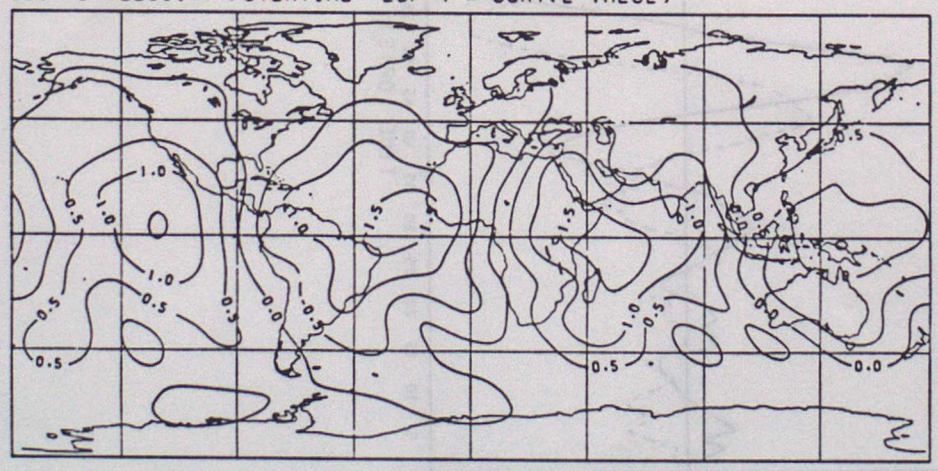

Figure 6c

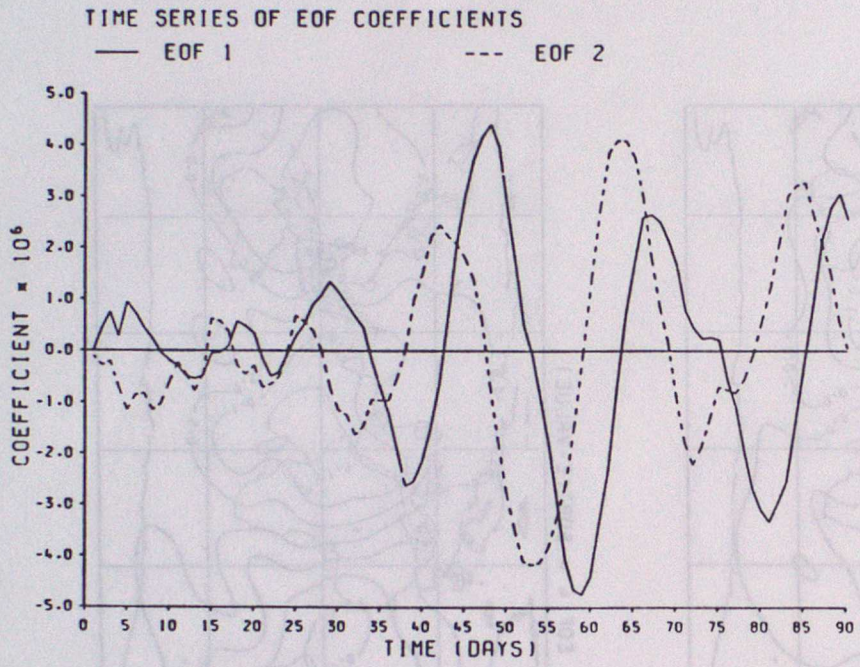
TIME SERIES OF EOF COEFFICIENTS
EOF 1
EOF 2
COEFFICIENT x 10⁶
5.0
4.0
3.0
2.0
1.0
0.0
-1.0
-2.0
-3.0
-4.0
-5.0
0
5
10
15
20
25
30
35
40
45
50
55
60
65
70
75
80
85
90
TIME (DAYS)

Figure 7

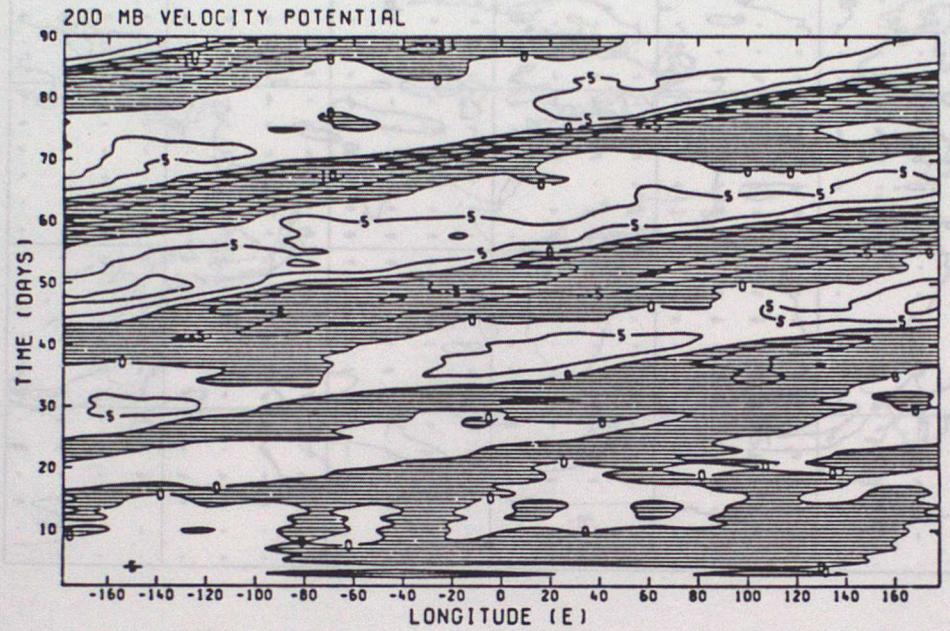
200 MB VELOCITY POTENTIAL
TIME (DAYS)
LONGITUDE (E)

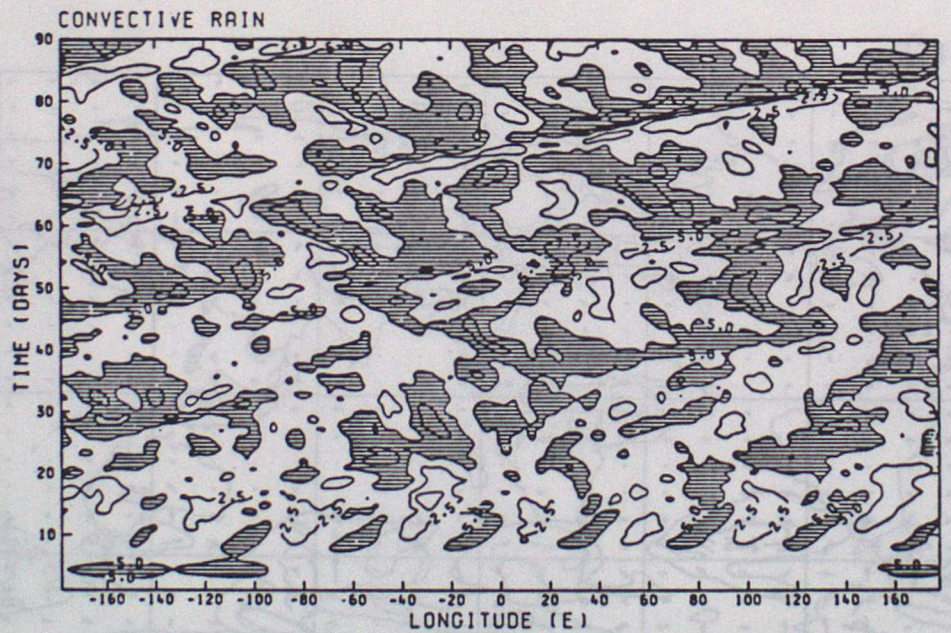
CONVECTIVE RAIN
TIME (DAYS)
LONGITUDE (E)

Figure 8

200 MB WIND COMPOSITE

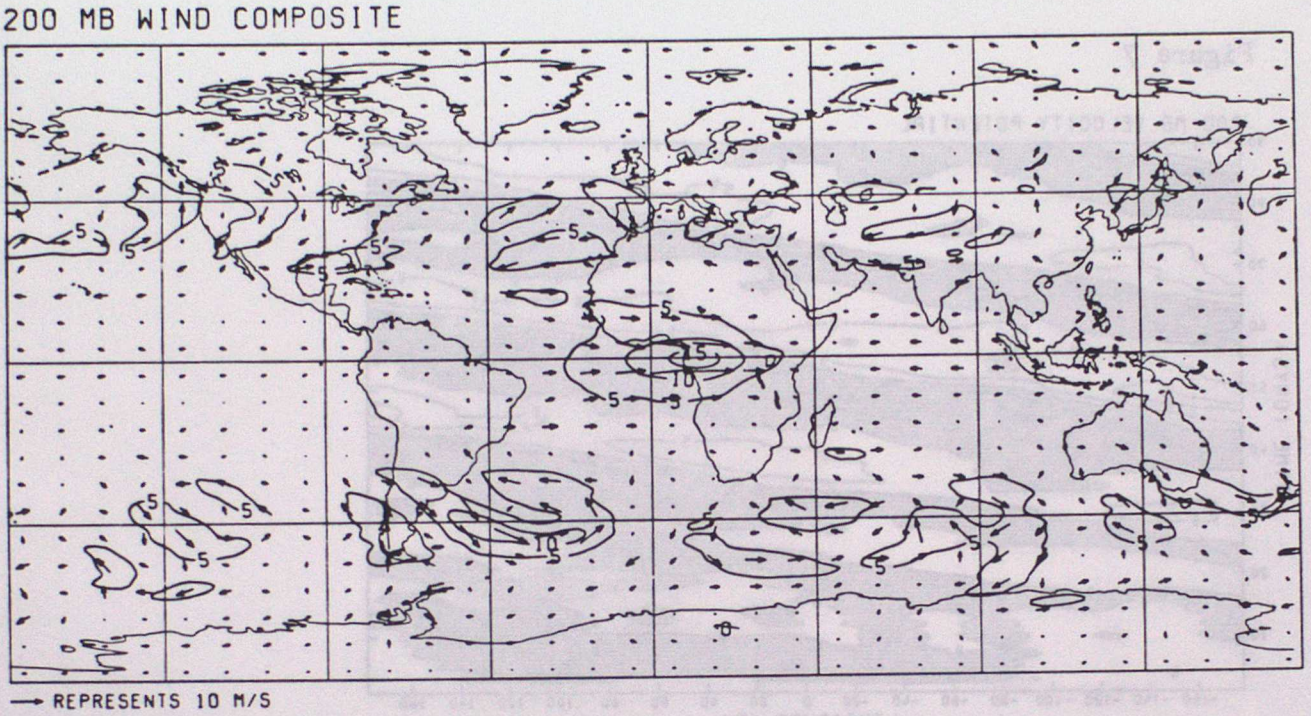

→ REPRESENTS 10 M/S

850 MB WIND COMPOSITE

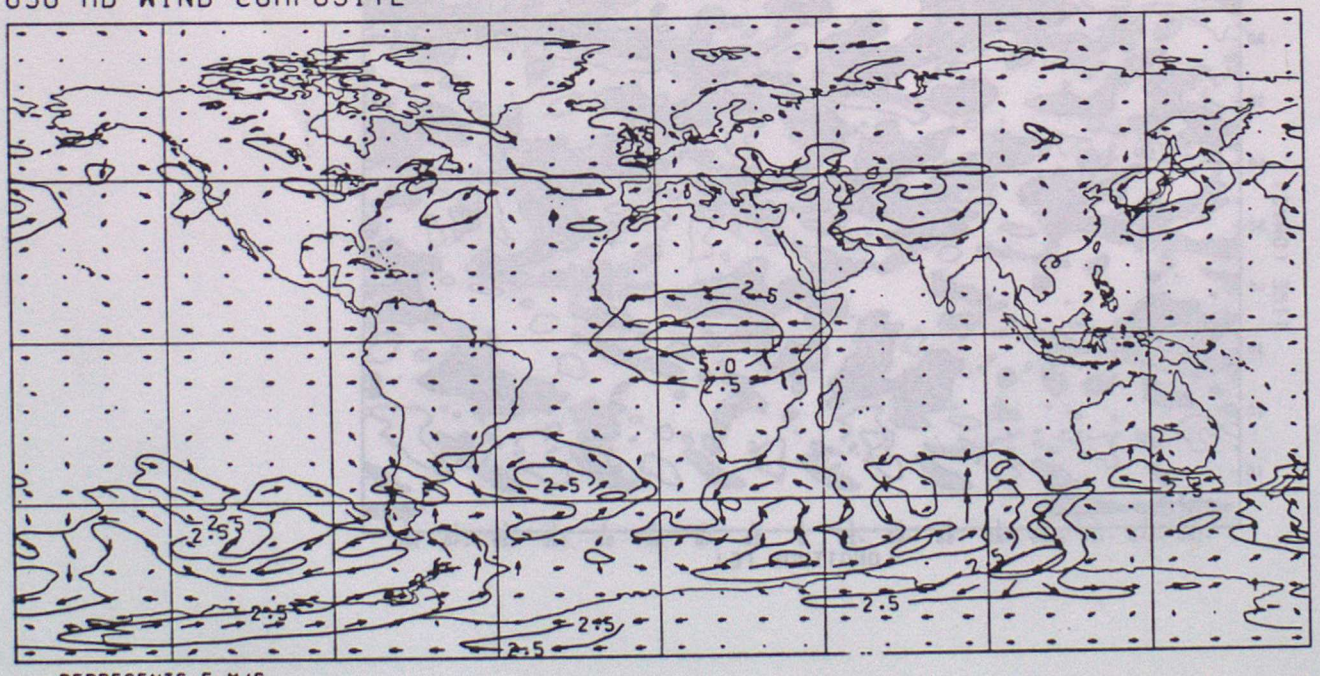

→ REPRESENTS 5 M/S

Figure 9

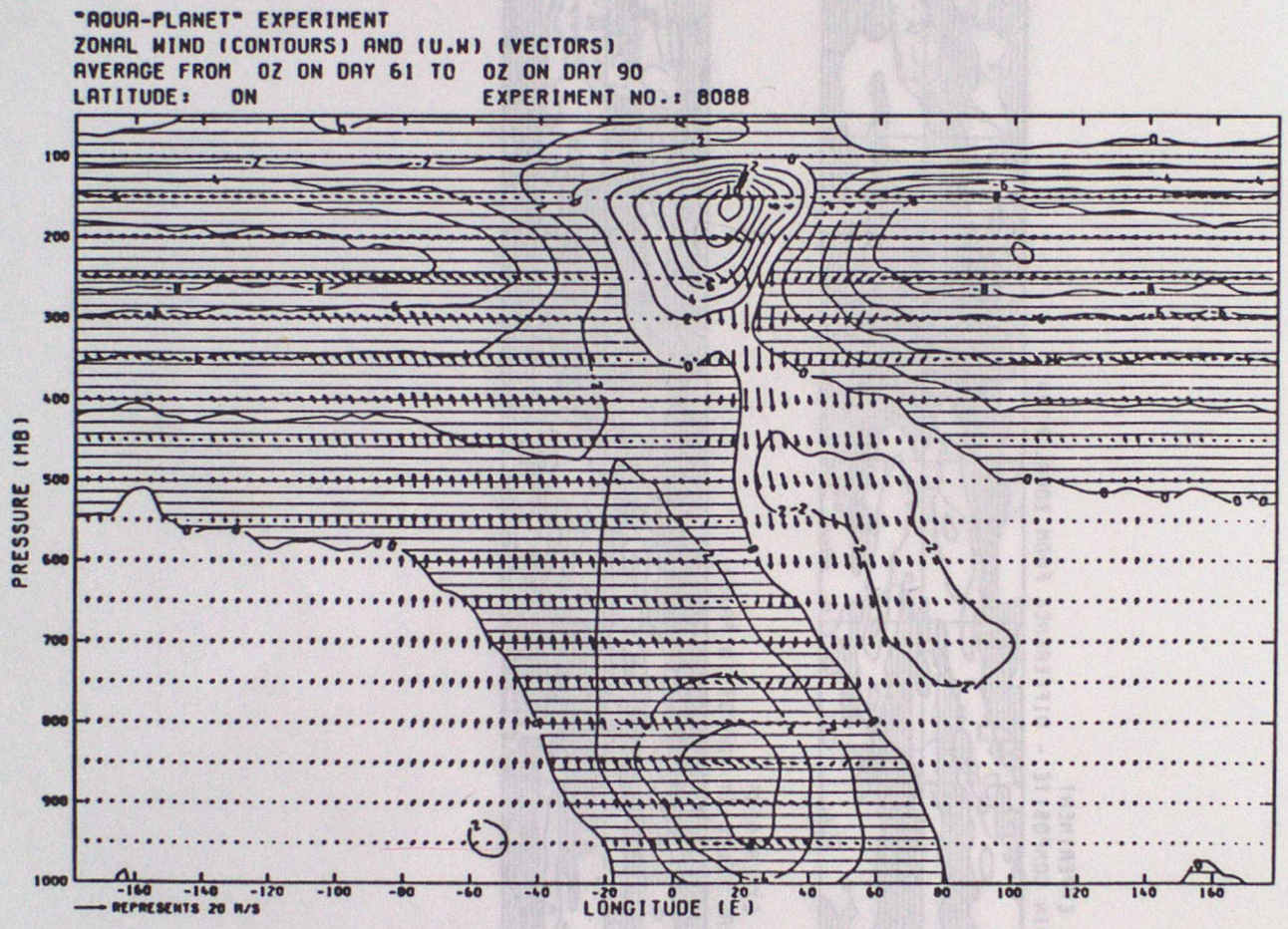
"AQUA-PLANET" EXPERIMENT
ZONAL WIND (CONTOURS) AND (U,W) (VECTORS)
AVERAGE FROM 0Z ON DAY 61 TO 0Z ON DAY 90
LATITUDE: ON
EXPERIMENT NO.: 8088
PRESSURE (MB)
100
200
300
400
500
600
700
800
900
1000
-160 -140 -120 -100 -80 -60 -40 -20 0 20 40 60 80 100 120 140 160
LONGITUDE (E)
REPRESENTS 20 M/S

Figure 10

"AQUA-PLANET" EXPERIMENT
CONVECTIVE RAIN COMPOSITE - DIFFERENCE FROM ZONAL MEAN

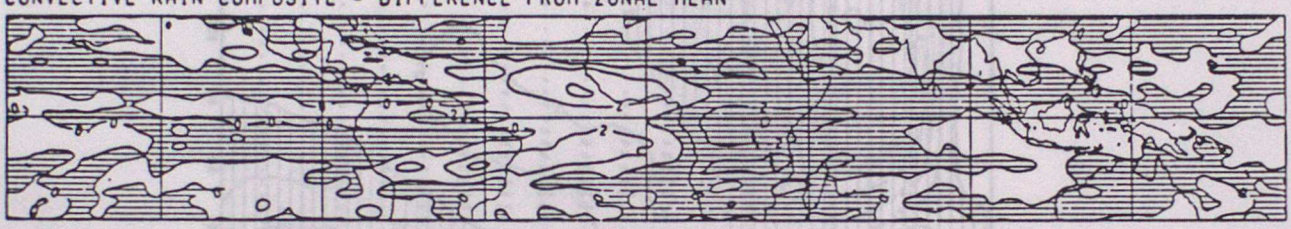

"AQUA-PLANET" EXPERIMENT
500 MB VERTICAL VELOCITY (DP/DT IN PA/S)

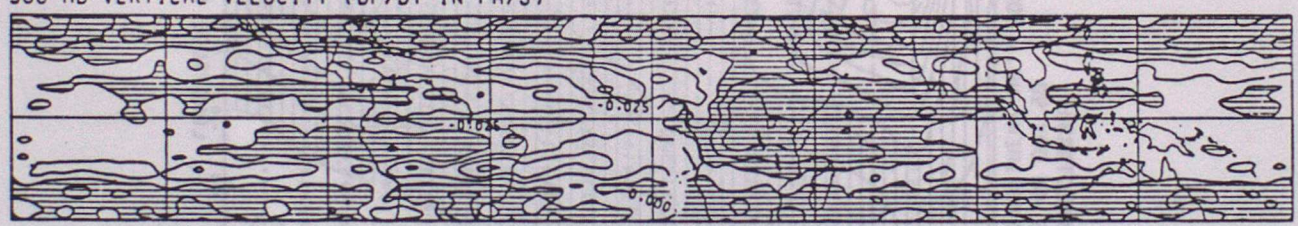

Figure 11

EXPT. WITH INCREASED TROPICAL SST
PRECIPITATION

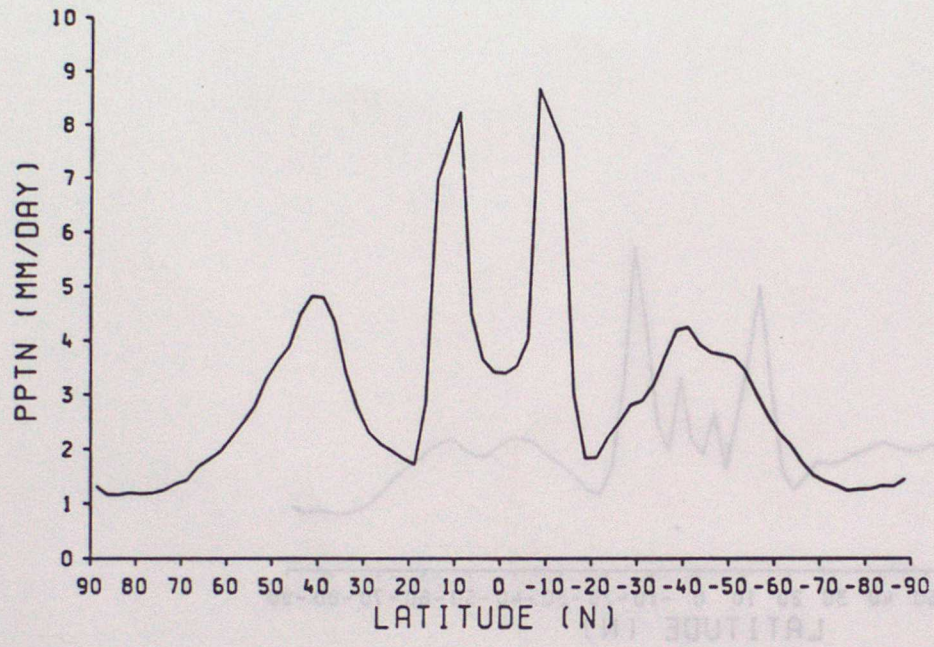

EXPT. WITH INCREASED TROPICAL SST
850 MB WESTERLY WIND

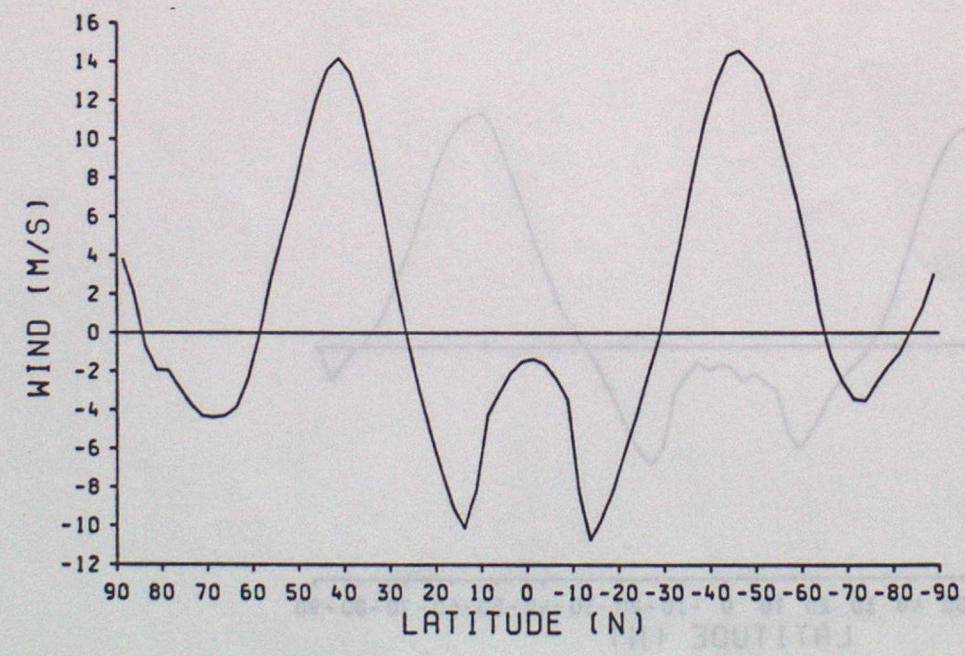

Figure 12

EXPT. WITH DOUBLED LATENT HEAT CONSTANT
PRECIPITATION

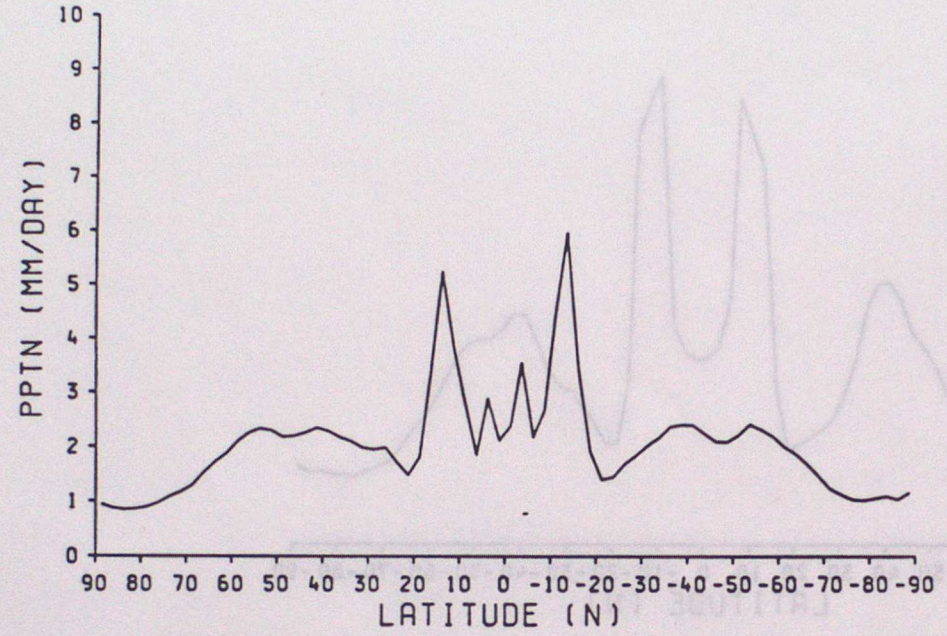

EXPT. WITH DOUBLED LATENT HEAT CONSTANT
850 MB WESTERLY WIND

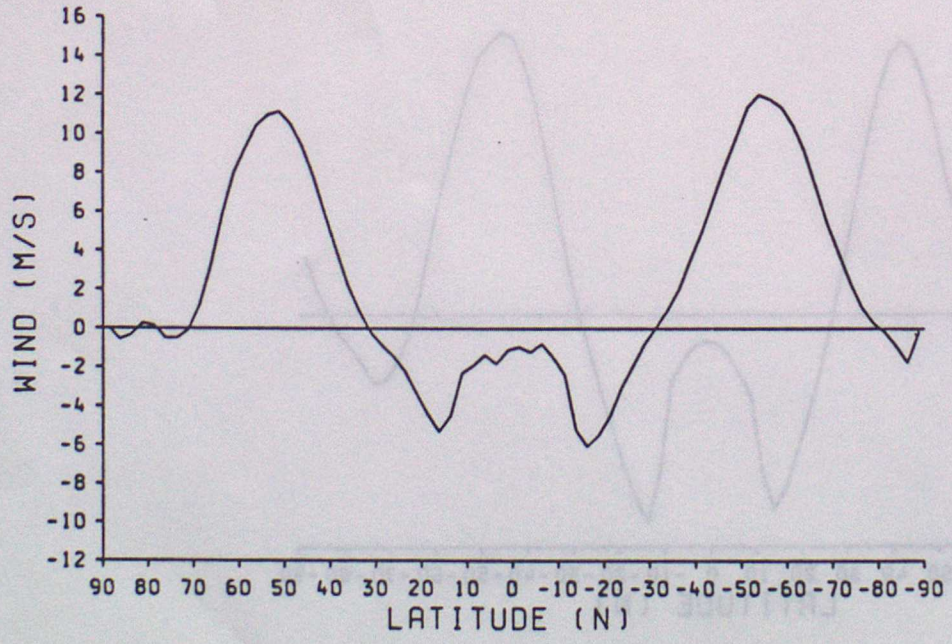

Figure 13

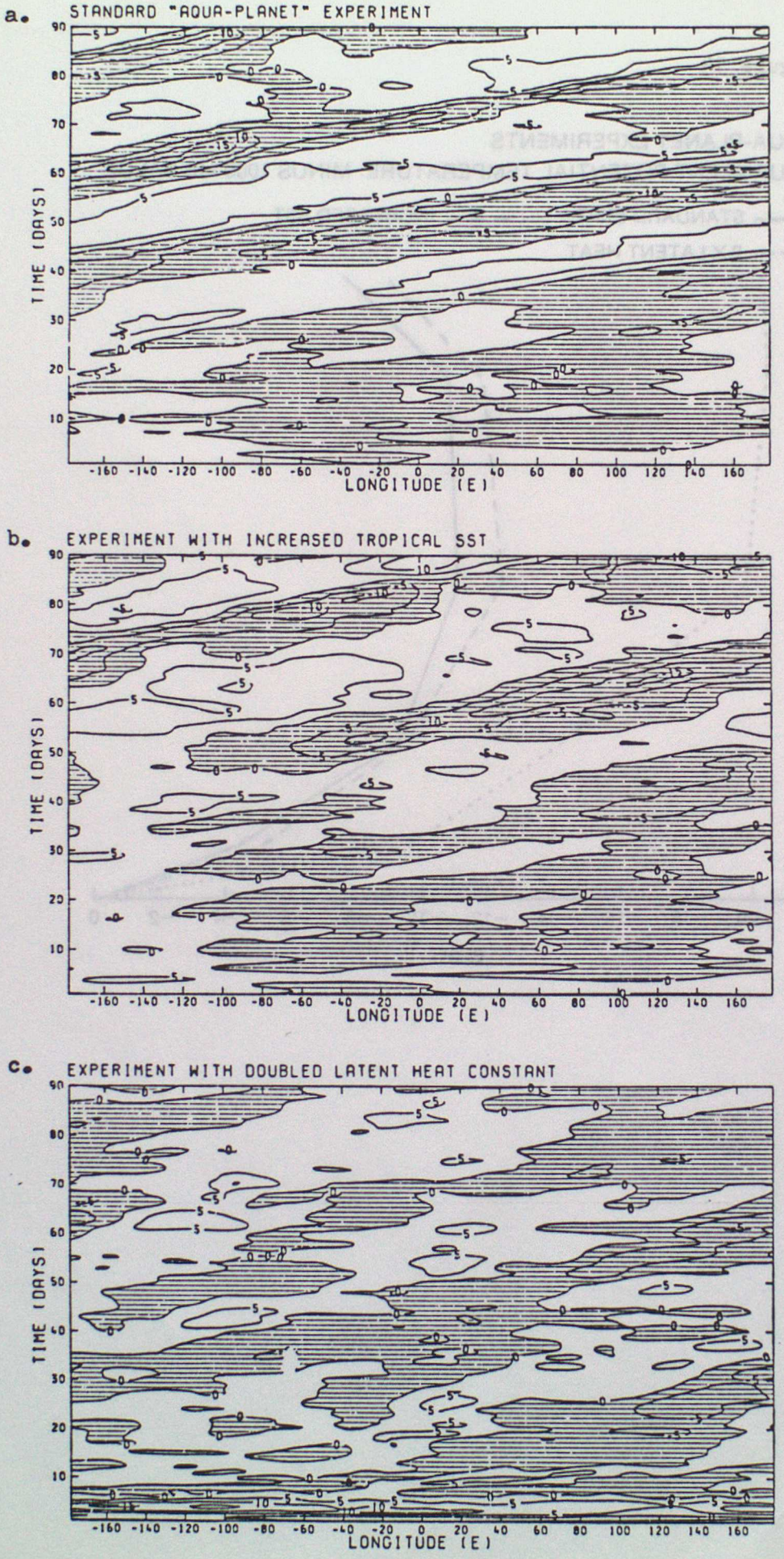
a.
STANDARD "AQUA-PLANET" EXPERIMENT
b.
EXPERIMENT WITH INCREASED TROPICAL SST
c.
EXPERIMENT WITH DOUBLED LATENT HEAT CONSTANT
TIME (DAYS)
LONGITUDE (E)

Figure 14

AQUA-PLANET EXPERIMENTS
EQUIVALENT POTENTIAL TEMPERATURE MINUS 1000 MB VALUE

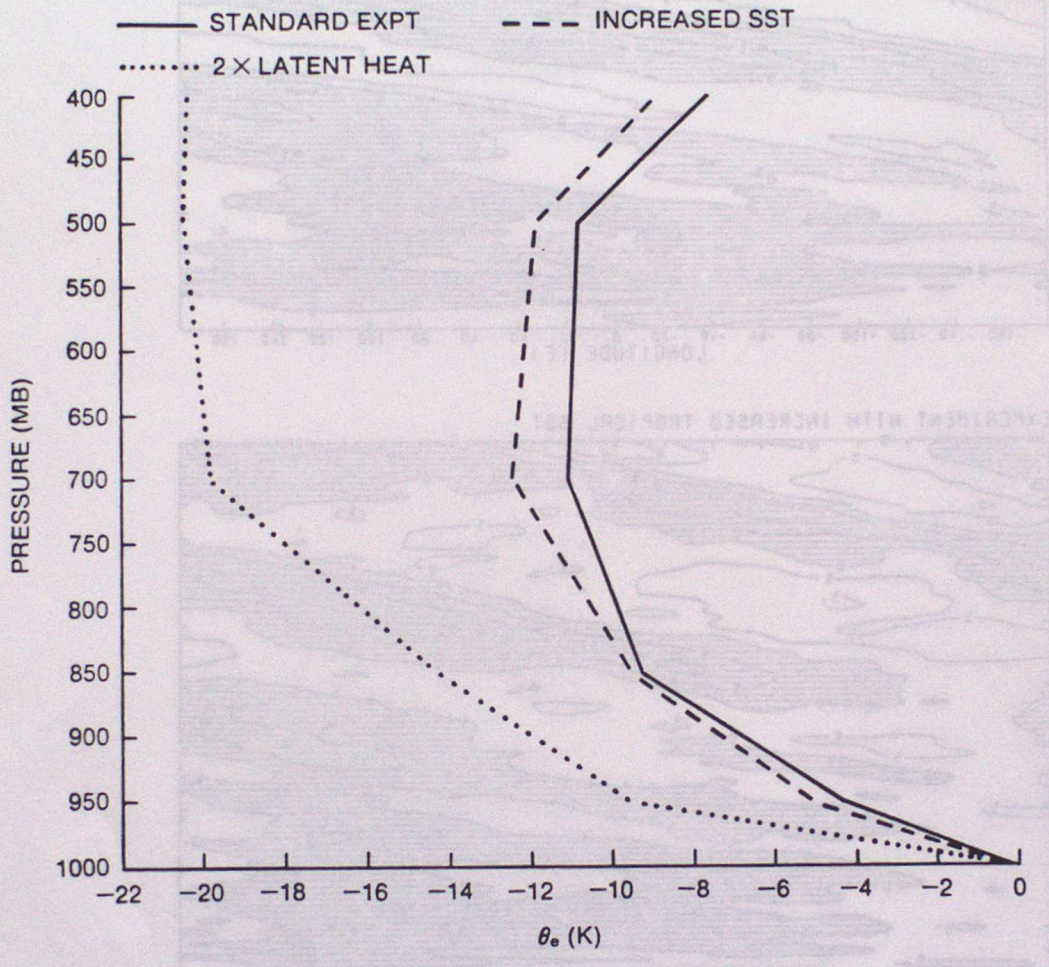

Figure 15

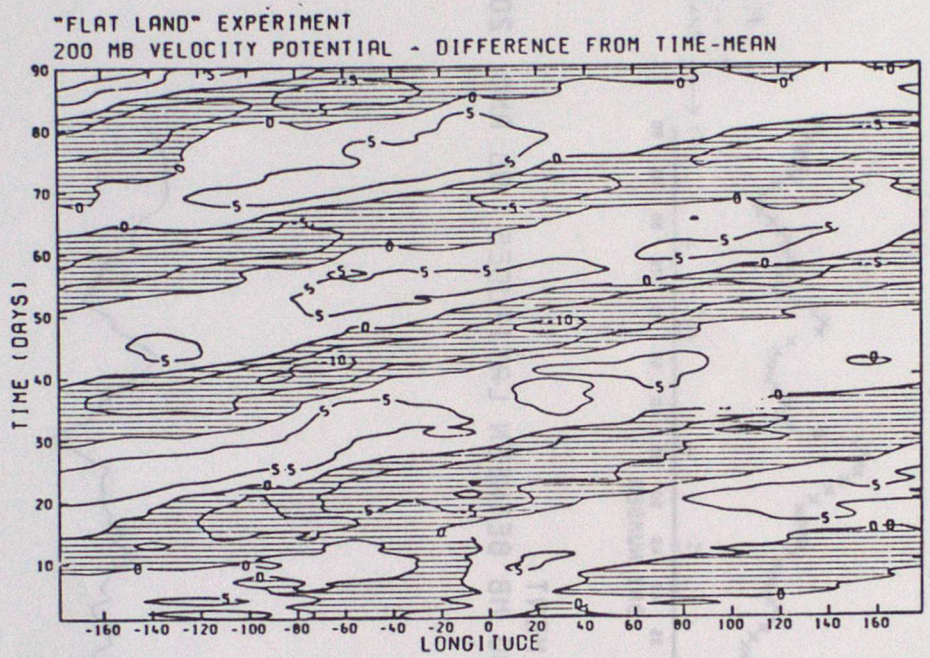
"FLAT LAND" EXPERIMENT
200 MB VELOCITY POTENTIAL - DIFFERENCE FROM TIME-MEAN
TIME (DAYS)
90
80
70
60
50
40
30
20
10
-160 -140 -120 -100 -80 -60 -40 -20 0 20 40 60 80 100 120 140 160
LONGITUDE

Figure 16

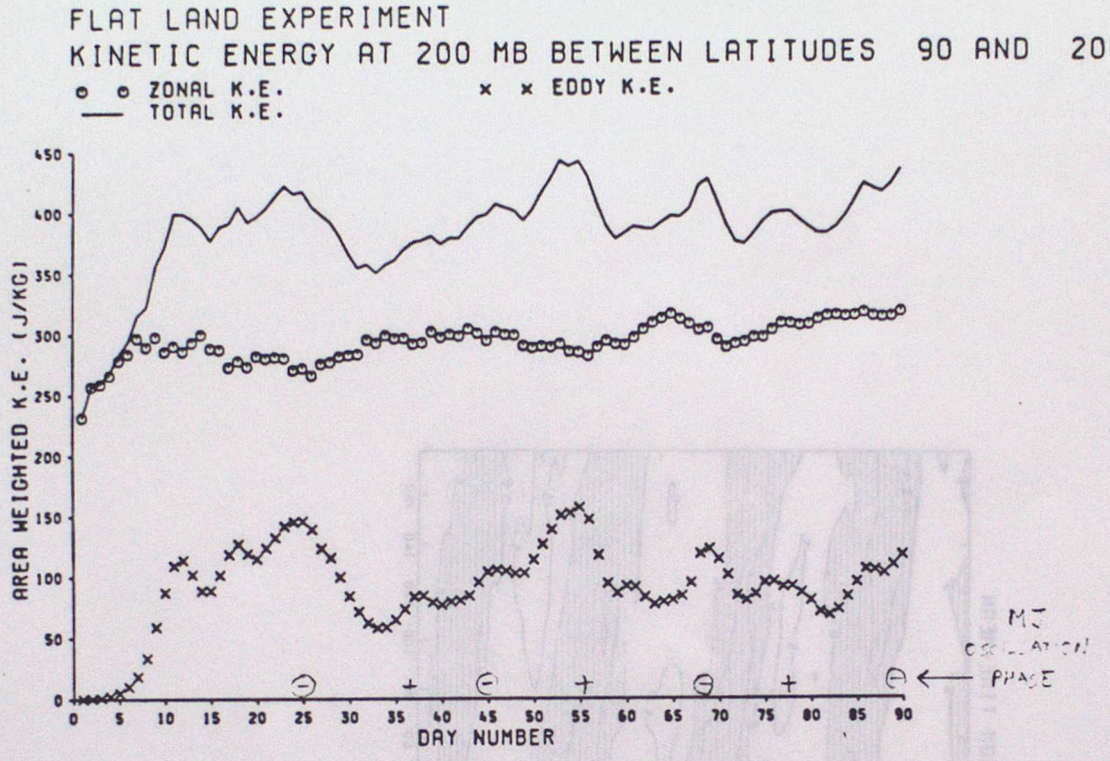
FLAT LAND EXPERIMENT
KINETIC ENERGY AT 200 MB BETWEEN LATITUDES 90 AND 20
o o ZONAL K.E.
x x EDDY K.E.
TOTAL K.E.
AREA WEIGHTED K.E. (J/KG)
DAY NUMBER
PHASE

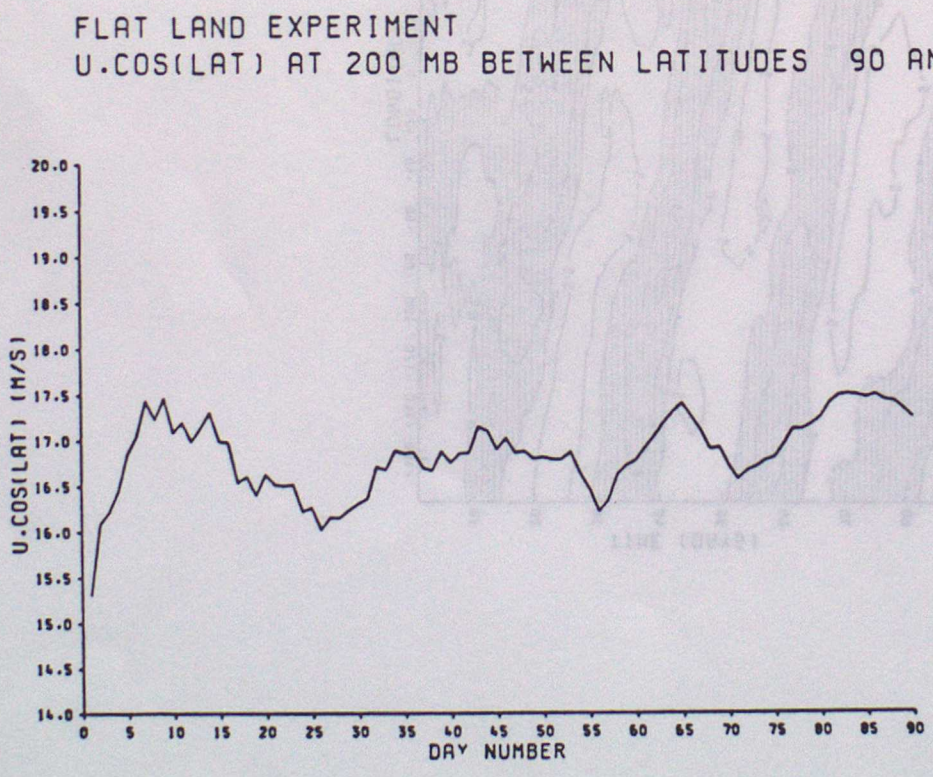
FLAT LAND EXPERIMENT
U.COS(LAT) AT 200 MB BETWEEN LATITUDES 90 AND 20
U.COS(LAT) (M/S)
DAY NUMBER

Figure 17

FLAT LAND EXPERIMENT
KINETIC ENERGY AT 200 MB BETWEEN LATITUDES -20 AND -90

o o ZONAL K.E. × × EDDY K.E.
—— TOTAL K.E.

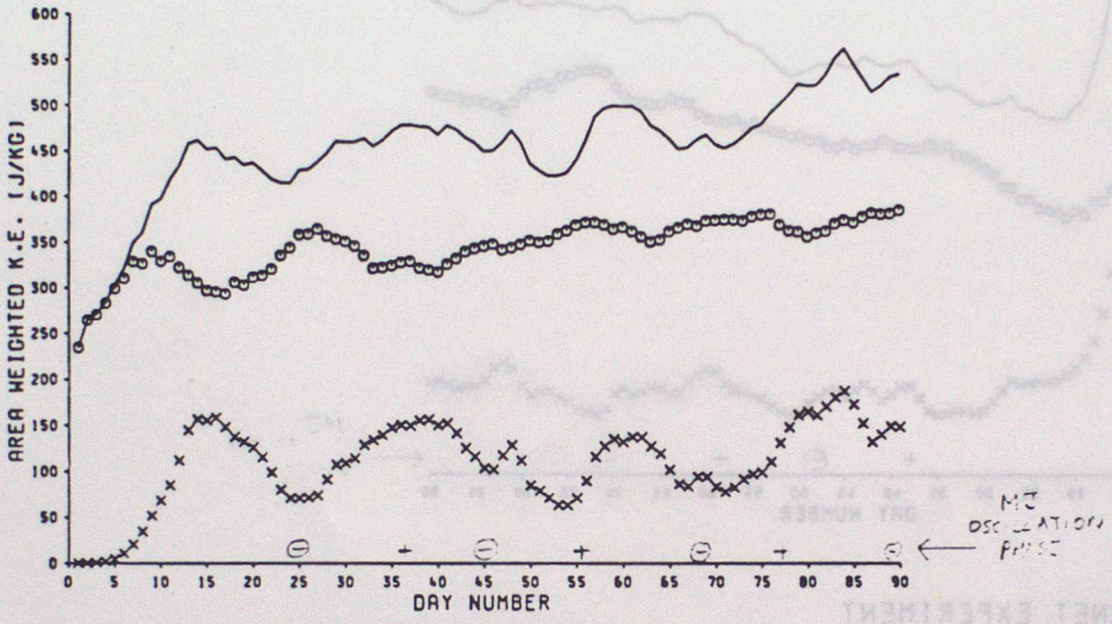

FLAT LAND EXPERIMENT
U.COS(LAT) AT 200 MB BETWEEN LATITUDES -20 AND -90

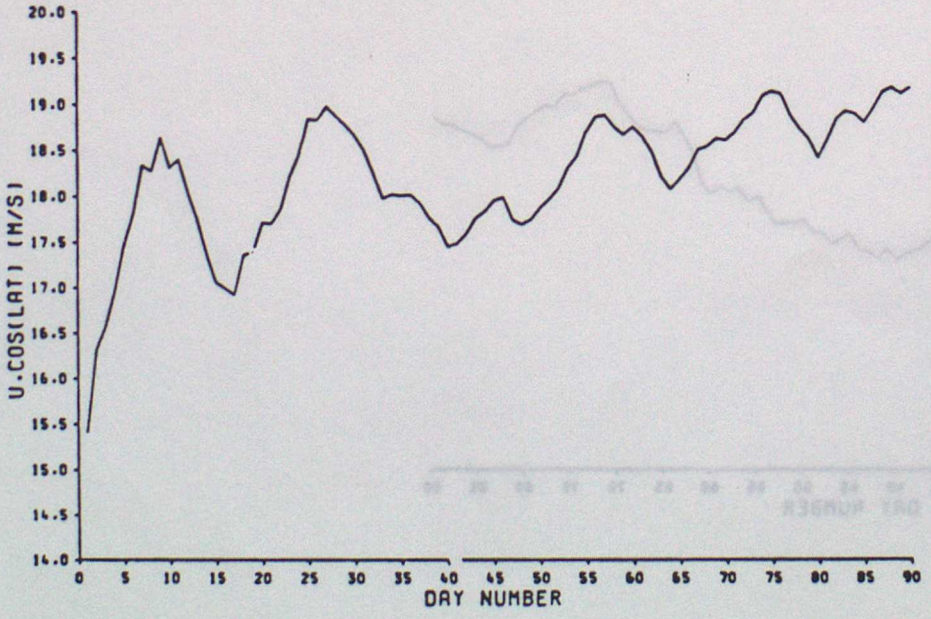

Figure 18

AQUA PLANET EXPERIMENT
KINETIC ENERGY AT 200 MB BETWEEN LATITUDES 90 AND 20

o o ZONAL K.E. × × EDDY K.E.
—— TOTAL K.E.

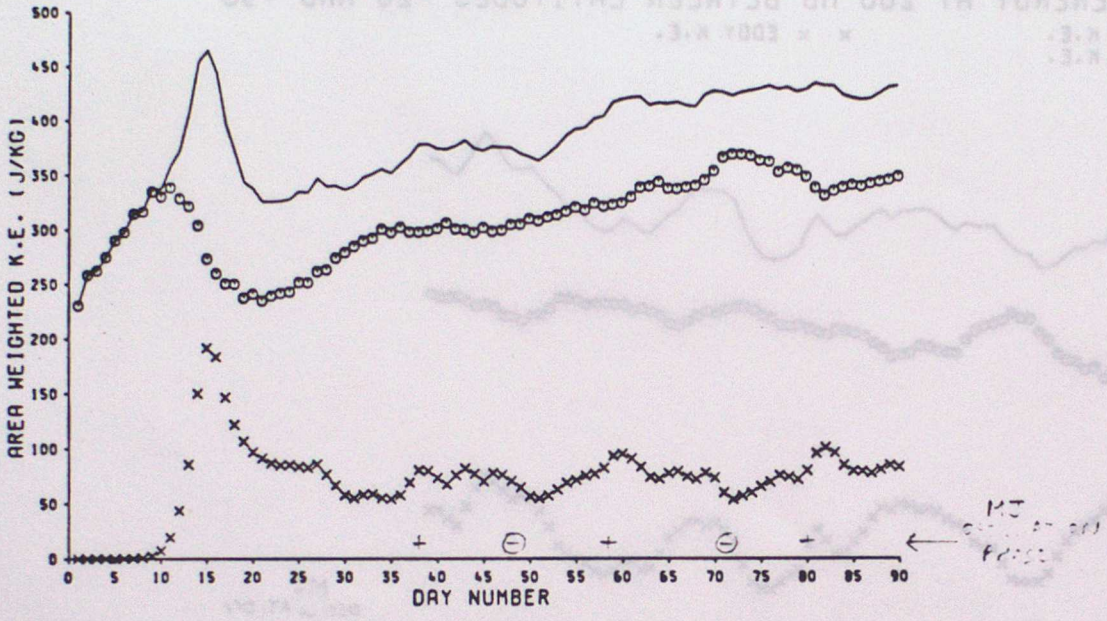

AQUA PLANET EXPERIMENT
U.COS(LAT) AT 200 MB BETWEEN LATITUDES 90 AND 20

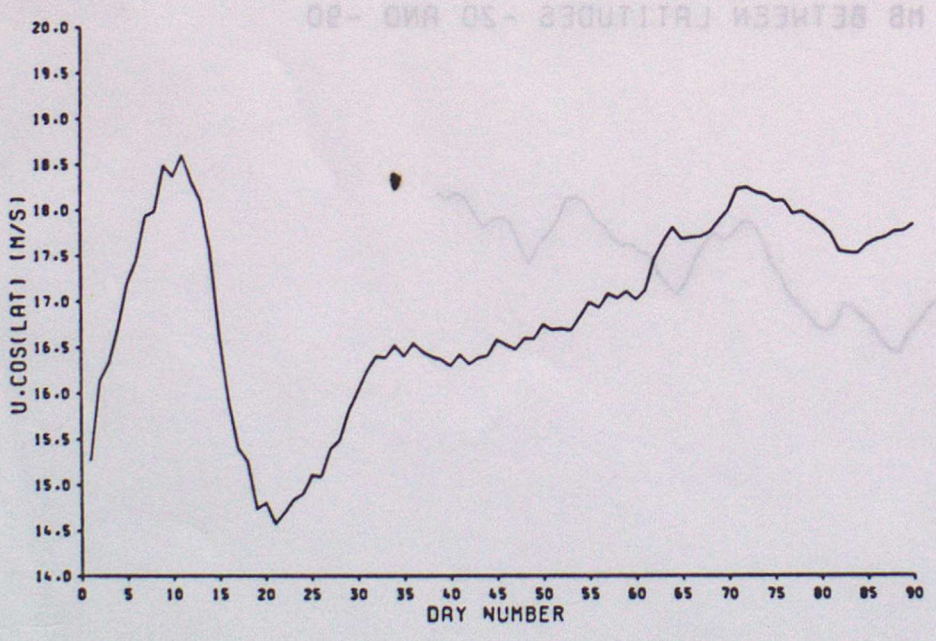

Figure 19

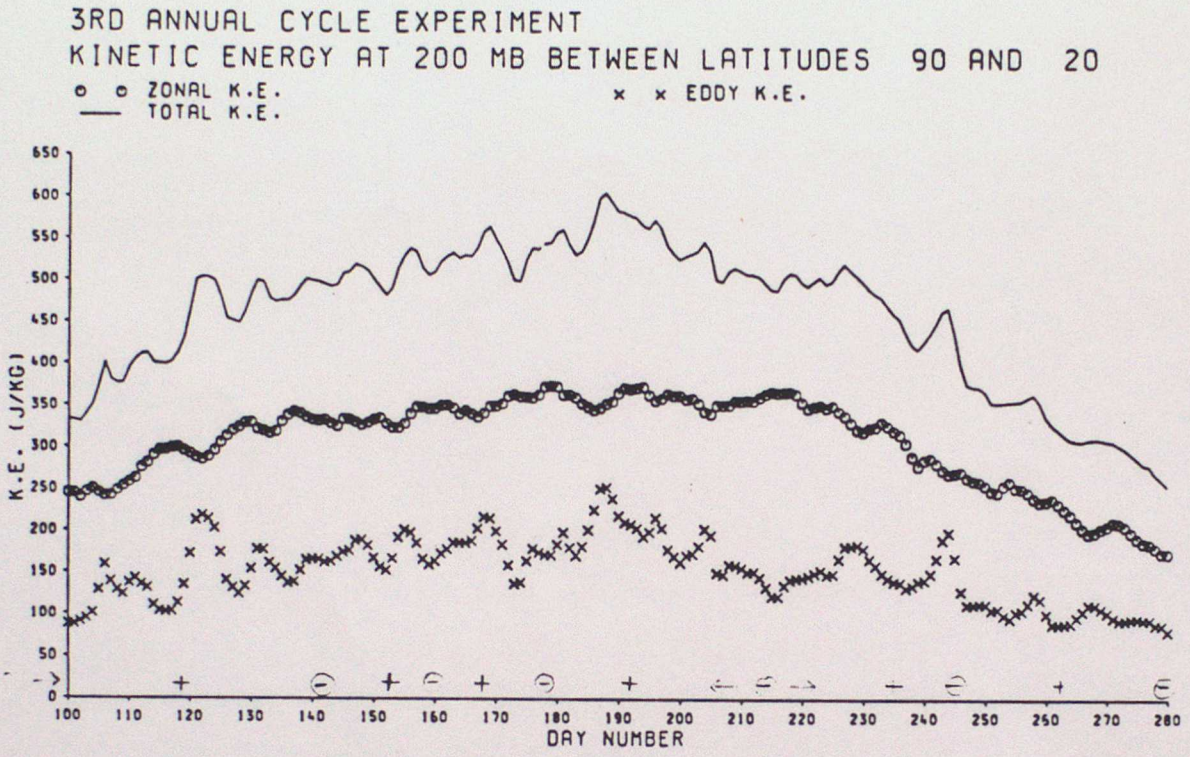
3RD ANNUAL CYCLE EXPERIMENT
KINETIC ENERGY AT 200 MB BETWEEN LATITUDES 90 AND 20
o o ZONAL K.E.
TOTAL K.E.
x x EDDY K.E.
K.E. (J/KG)
650
600
550
500
450
400
350
300
250
200
150
100
50
0
100 110 120 130 140 150 160 170 180 190 200 210 220 230 240 250 260 270 280
DAY NUMBER

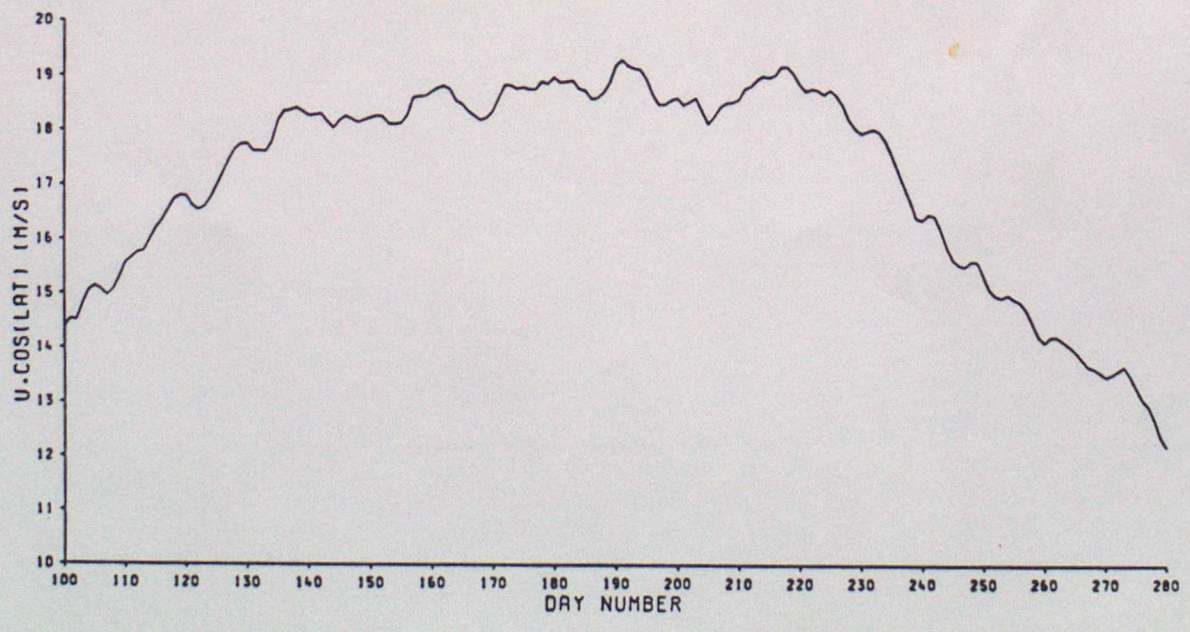
3RD ANNUAL CYCLE EXPERIMENT
U.COS(LAT) AT 200 MB BETWEEN LATITUDES 90 AND 20
U.COS(LAT) (M/S)
20
19
18
17
16
15
14
13
12
11
10
100 110 120 130 140 150 160 170 180 190 200 210 220 230 240 250 260 270 280
DAY NUMBER

INDEX TO LONG-RANGE FORECASTING AND CLIMATE RESEARCH SERIES

1. THE CLIMATE OF THE WORLD - Introduction and description of world climate.
by C K Folland (March 1986)

2. THE CLIMATE OF THE WORLD - Forcing and feedback processess.
by C K Folland (March 1986)

3. THE CLIMATE OF THE WORLD - El Nino/Southern Oscillation and the Quasi-biennial Oscillation.
by C K Folland and D E Parker (March 1986)

4. THE CLIMATE OF THE WORLD - Climate change: the ancient earth to the 'Little Ice Age'.
by C K Folland (March 1986)

5. THE CLIMATE OF THE WORLD - Climate Change: the instrumental period.
by C K Folland and D E Parker (March 1986)

6. THE CLIMATE OF THE WORLD - Carbon dioxide and climate (with appendix on simple climate models).
by D E Parker, C K Folland and D J Carson (March 1986)

7. Sahel rainfall, Northern Hemisphere circulation anomalies and worldwide sea temperature changes. (To be published in the Proceedings of the "Pontifical Academy of Sciences Study Week", Vatican, 23-27 September 1986).
by C K Folland, D E Parker, M N Ward and A W Colman (September 1986)

8. Lagged-average forecast experiments with a 5-level general circulation model.
by J M Murphy (March 1986)

9. Statistical Aspects of Ensemble Forecasts.
by J M Murphy (July 1986)

10. The Impact of El Nino on an Ensemble of Extended-Range Forecasts. (Submitted to Monthly Weather Review)
by J A Owen and T N Palmer (December 1986)

11. An experimental forecast of the 1987 rainfall in the Northern Nordeste region of Brazil.
by M N Ward, S Brooks and C K Folland (March 1987)

12. The Sensitivity of Estimates of Trends of Global and Hemisphere Marine Temperature to Limitations in Geographical Coverage.
by D E Parker (April 1987)

13. General circulation model simulations using cloud distributions from the GAPOD satellite data archive and other sources.
by R Swinbank (May 1987)

14. Simulation of the Madden and Julian Oscillation in GCM experiments.
by R Swinbank (May 1987)